Experimental Studies of Radiation and Plasma Effects behind the Incident Shock in LENS XX, and the Unsteady Flow Characteristics associated with "Free Flight" Shroud and Stage Separation and Mode Switching in LENS II

Michael S. Holden, PhD
CUBRC, Inc.
4455 Genesee Street
Buffalo, NY 14225, USA

holden@cubrc.org

1.0 OUTLINE

- Experimental studies of radiation and plasma effects behind the incident shock in LENS XX
- Shroud and Stage Separation Studies in LENS II Shock Tunnel
- Foam and ice debris studies for the NASA Shuttle Return-to-Flight Program in LENS II
- Fundamental studies of unsteady flow phenomena associated with starting door and mode switching for Ramjet and Scramjet engines
- Summary

2.0 EXPERIMENTAL STUDIES OF RADIATION AND PLASMA EFFECTS BEHIND THE INCIDENT SHOCK IN LENS XX

The LENS XX facility was developed principally to generate clean hypervelocity flows in which we can perform experiments to evaluate nonequilibrium and real gas effects in the shock layers surrounding vehicles flown at velocities from 3 km/s to 14 km/s, and to study shock layer radiation and the properties of plasmas surrounding hypersonic vehicles as they enter the earth's atmosphere and those of other planets. Currently our research is directed toward examining the radiation behind a shock front traveling at 10 km/s for direct comparison with measurements made in East Facility at NASA Ames and developing a test program to obtain ground test measurements to directly compare with measurements made earlier in flight in the FIRE-II and RAM-C programs. Spectrographic measurements of the radiation behind a shock wave traveling at 10 km/s are being conducted in the expansion tube section of the LENS XX tunnel while those to replicate flight data are being made in the test section of the LENS XX facility as illustrated in Figure 1(a) and (b) respectively.

Report Documentation Page

Form Approved
OMB No. 0704-0188

1. REPORT DATE	2. REPORT TYPE	3. DATES COVERED
APR 2010	**N/A**	**-**

4. TITLE AND SUBTITLE

Experimental Studies of Radiation and Plasma Effects behind the Incident Shock in LENS XX, and the Unsteady Flow Characteristics associated with Free Flight Shroud and Stage Separation and Mode Switching in LENS II

5a. CONTRACT NUMBER

5b. GRANT NUMBER

5c. PROGRAM ELEMENT NUMBER

6. AUTHOR(S)

5d. PROJECT NUMBER

5e. TASK NUMBER

5f. WORK UNIT NUMBER

7. PERFORMING ORGANIZATION NAME(S) AND ADDRESS(ES)

CUBRC, Inc. 4455 Genesee Street Buffalo, NY 14225, USA

8. PERFORMING ORGANIZATION REPORT NUMBER

9. SPONSORING/MONITORING AGENCY NAME(S) AND ADDRESS(ES)

10. SPONSOR/MONITOR'S ACRONYM(S)

11. SPONSOR/MONITOR'S REPORT NUMBER(S)

12. DISTRIBUTION/AVAILABILITY STATEMENT

Approved for public release, distribution unlimited

13. SUPPLEMENTARY NOTES

See also ADA569031. Aerothermodynamic Design, Review on Ground Testing and CFD (Conception aerothermodynamique, revue sur les essais au sol et dynamique des fluides informatisee).

14. ABSTRACT

15. SUBJECT TERMS

16. SECURITY CLASSIFICATION OF:			17. LIMITATION OF ABSTRACT	18. NUMBER OF PAGES	19a. NAME OF RESPONSIBLE PERSON
a. REPORT	b. ABSTRACT	c. THIS PAGE			
unclassified	**unclassified**	**unclassified**	**SAR**	**34**	

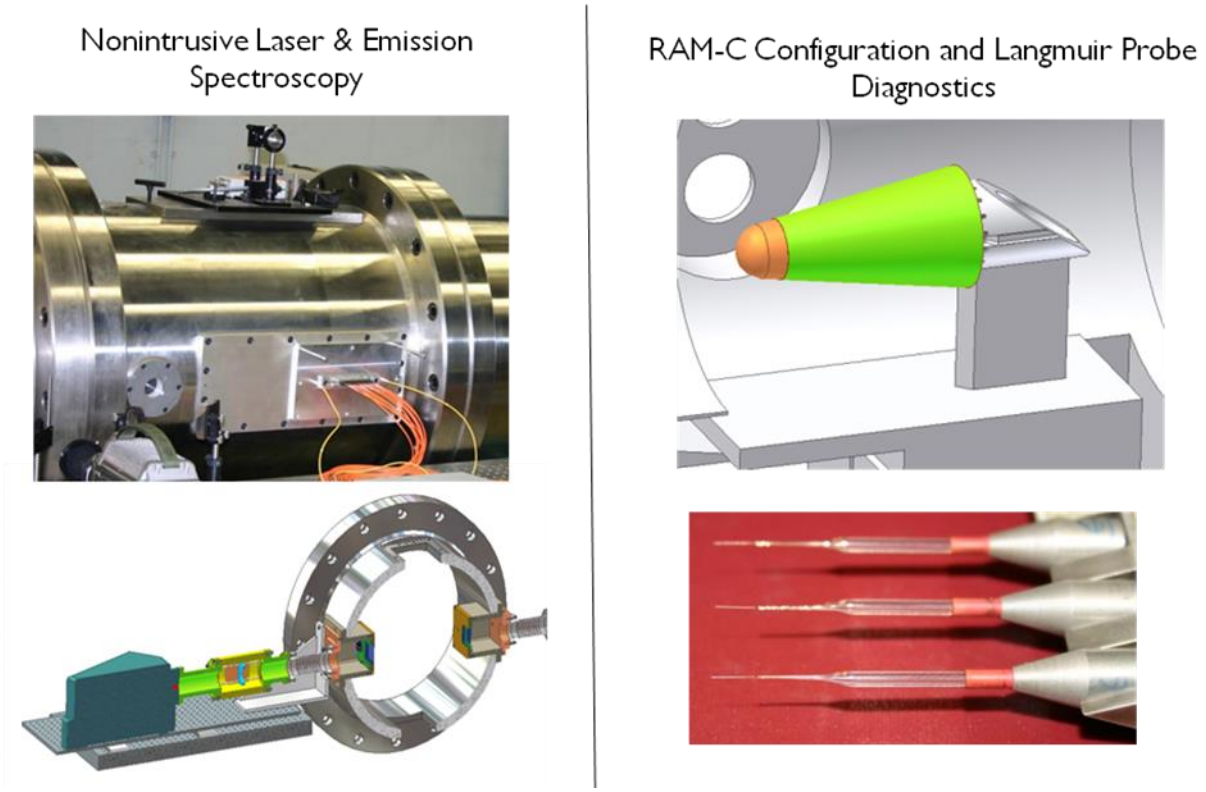

Figure 1: LENS XX Capability to Study Radiation and Plasma Effects

The instrumentation used in our studies in the expansion tube replicate those in the East Facility with spectrometers, radiometers, and monochrometers as well as laser diodes to accurately measure shock velocity. Figure 2 shows a photograph of the instrumentation setup on one side of the test section in the expansion tube. A summary of differences between the LENS XX expansion tunnel and the East Facility is listed in Figure 3. A major advantage of using the expansion tunnel to generate a strong shock is that the contamination levels are significantly less than those for a reflected shock tunnel. The 24-inch test section in the LENS XX facility is roughly five times larger than the East tunnel, allowing us to obtain measurements over significantly larger path lengths to potentially provide more accurate data. Because of the large size of the facility, we can afford to employ wedge-inserts for the windows such that we can eliminate all effects associated with the growth of large boundary layers.

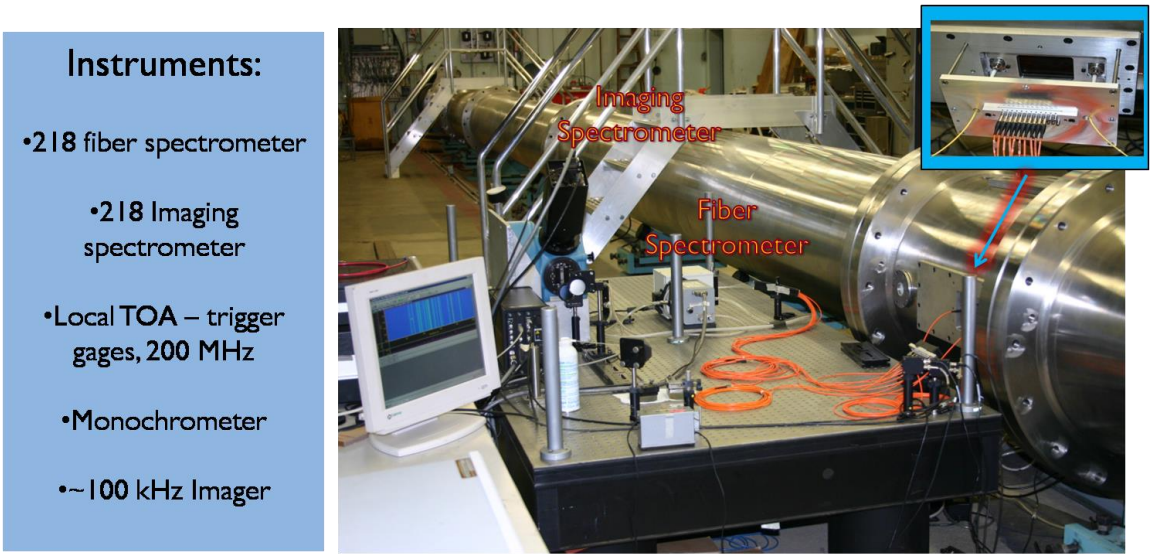

Figure 2: Optical Setup: South Side

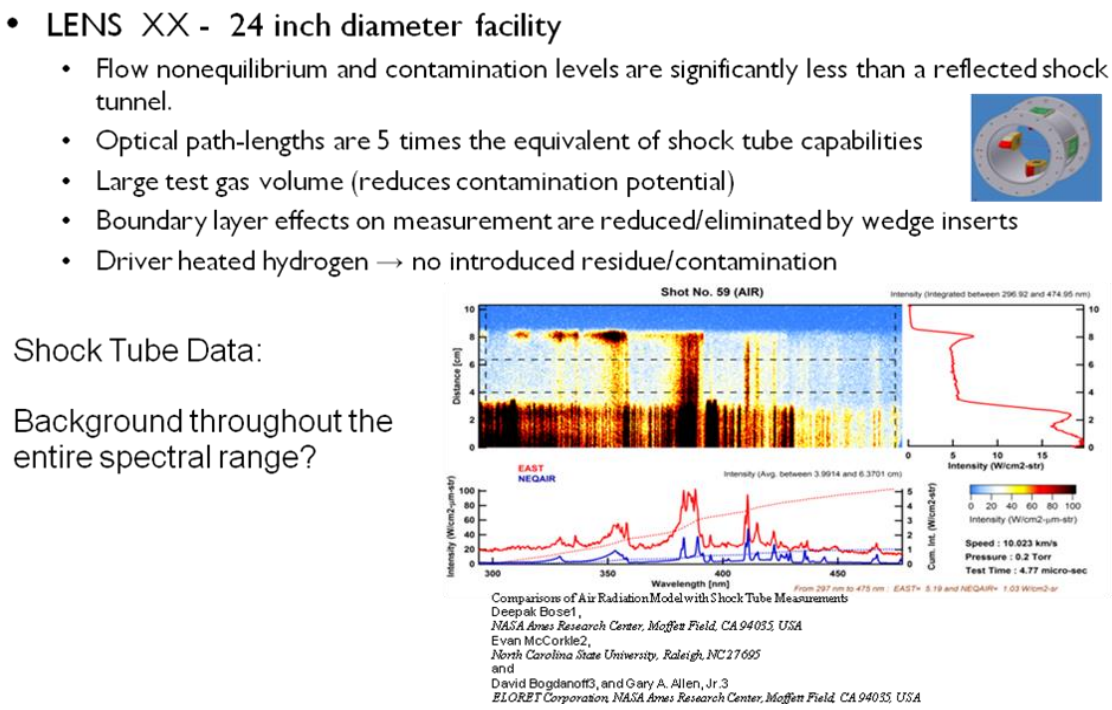

Figure 3: Summary of LENS XX Testing Environment for Radiation Studies

Using a heated hydrogen driver rather than the electrical discharge system employed in the East facility significantly reduces the contamination and clean up requirements. Also there is significantly less background radiation developed in the LENS XX tunnel. Figures 4, 5 and 6 illustrate further details of the arrangement of the instrumentation around the LENS XX expansion tube.

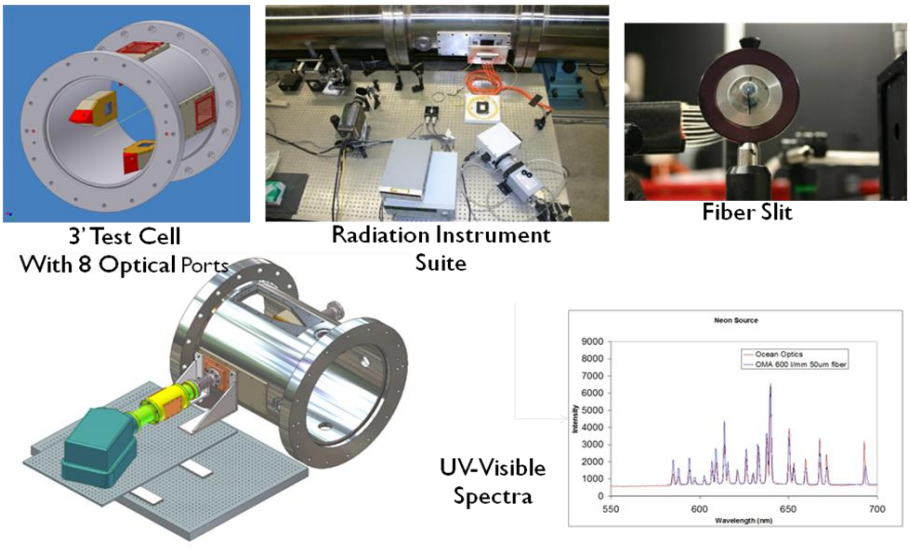

Figure 4: Radiation Spectroscopy Optical Bench Installed Adjacent to LENS XX

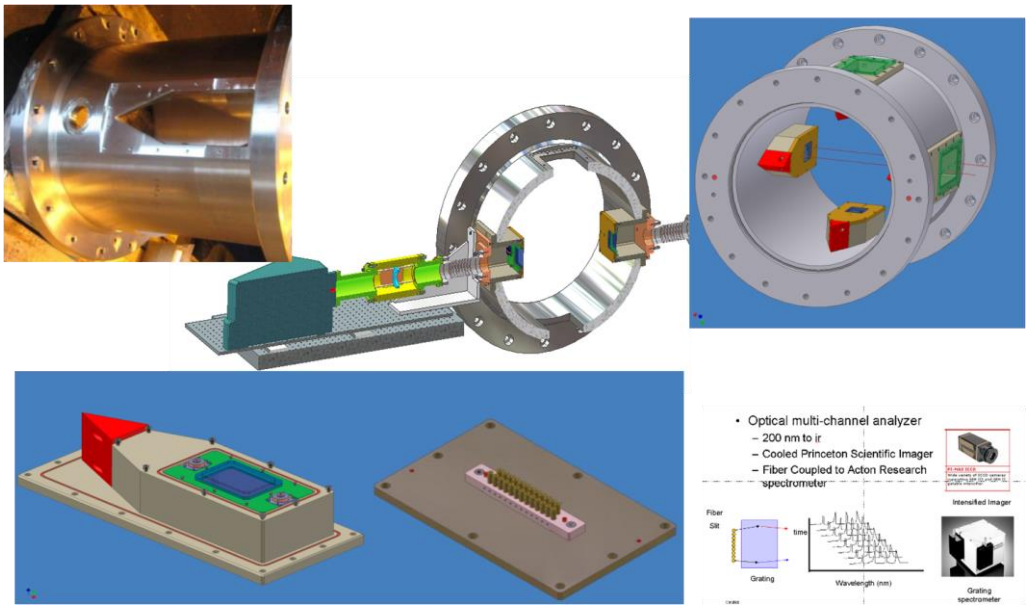

Figure 5: Two-Ft Diameter LENS XX Tube with Fiber Spectrometer Interface

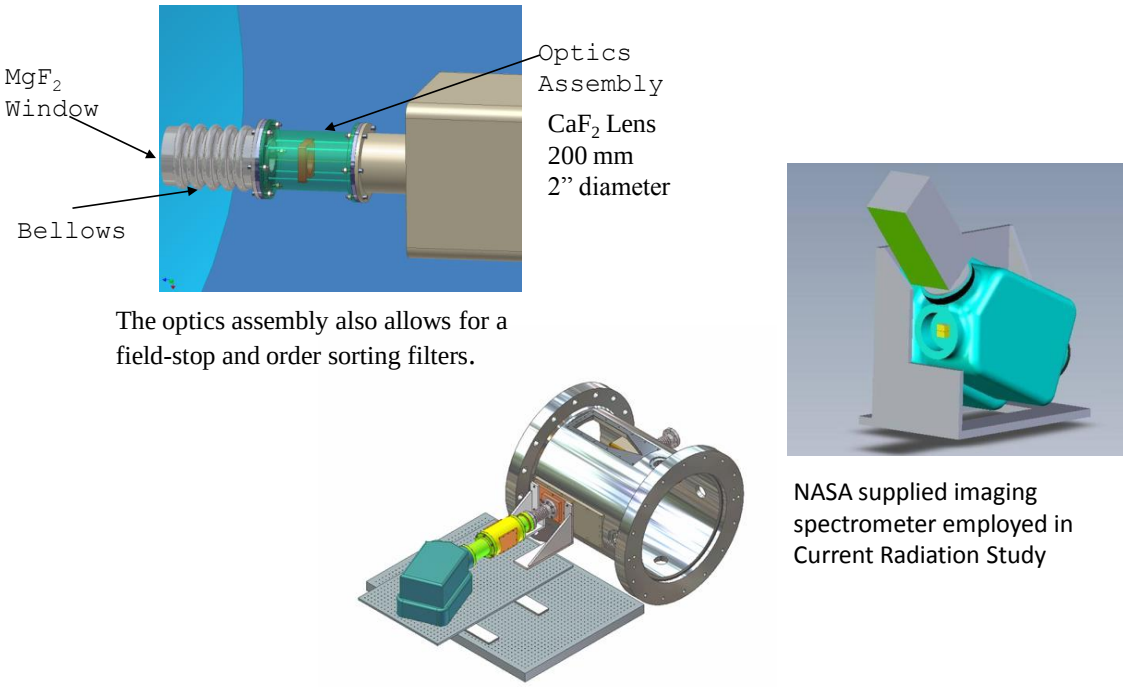

Figure 6: Vacuum UV Monochrometer Capabilities

Images of the shock front as it passes through the test section are shown in Figure 7.

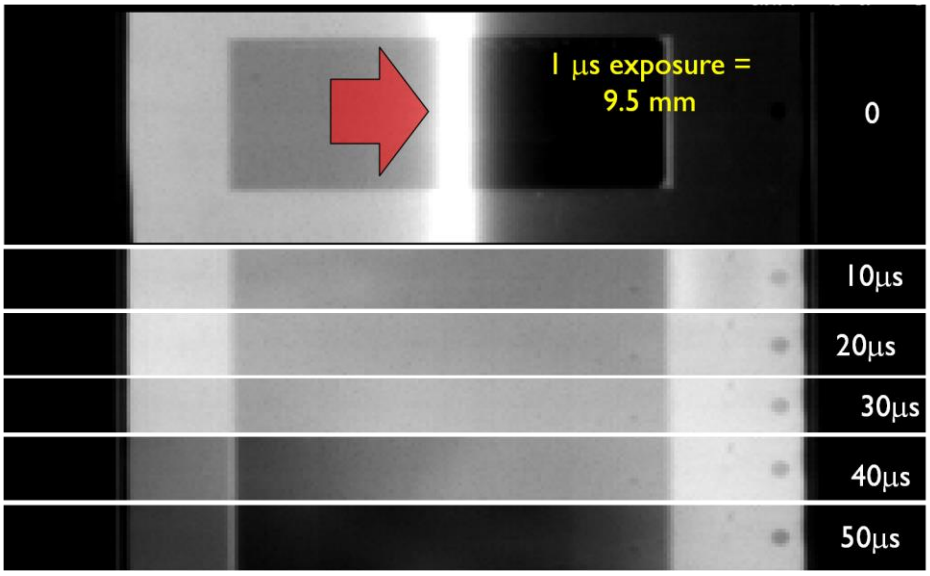

Figure 7: Shock Front Images (visible 300 – 1,000 nm)

Currently, we are making preparations to conduct two sets of experimental studies in the LENS XX test section to obtain radiation measurements in the shock layer over a replica of the FIRE-II capsule and obtain plasma measurements on the frustum of a full-scale RAM-C configuration using Langmuir probes and surface electrometers. The object in both of these studies is to provide significantly more accurate

measurements both at flight conditions and over a larger range of velocities with which to evaluate and improve the modeling of shock layer chemistry on the blunt nosetip and electron properties in the boundary layer on the frustum of a blunted cone configuration. The layout of the instrumentation that would be employed in the LENS XX studies which would replicate the instrumentation on the flight vehicle is illustrated in Figures 8 and 9. We plan to obtain radiation measurements with spectrometers viewed through the surface and positioned perpendicular to the flow viewing the shock layer from the side as illustrated in Figure 8. We also plan to measure radiation heating with thin-film instrumentation installed in the spherical heat shield together with calorimeter and thermocouple gages to examine catalytic heating effects.

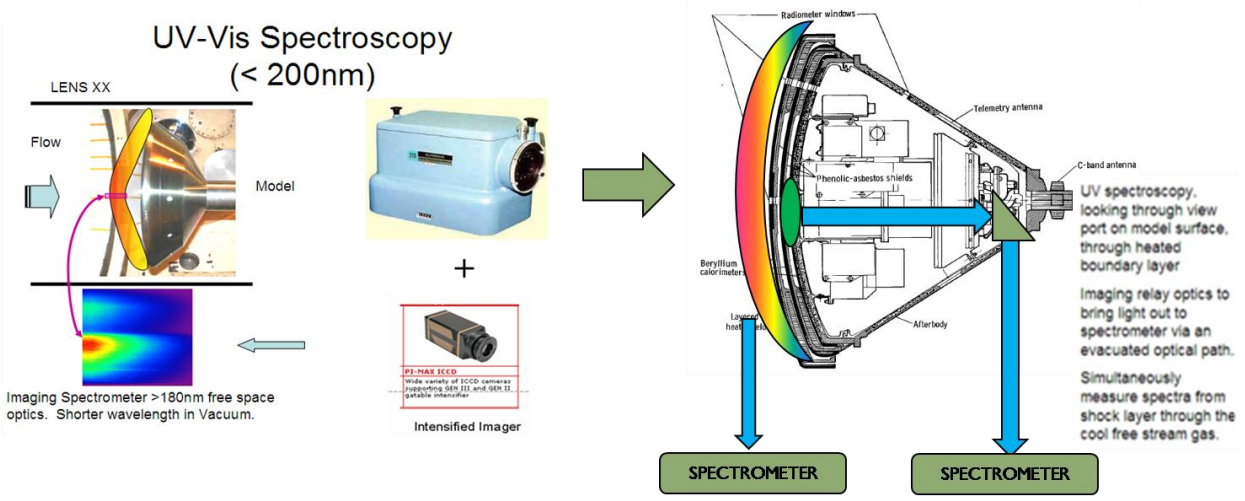

Spectroscopic measurements to be made using two techniques:

1) Emission perpendicular to flow looking at the shock layer from the side

2) Surface radiation spectroscopy viewed from a point on the surface measuring the net delivery from the optically thick gas

Figure 8: Proposed Shock Layer Radiation Measurements on Capsule Models (Fire II)

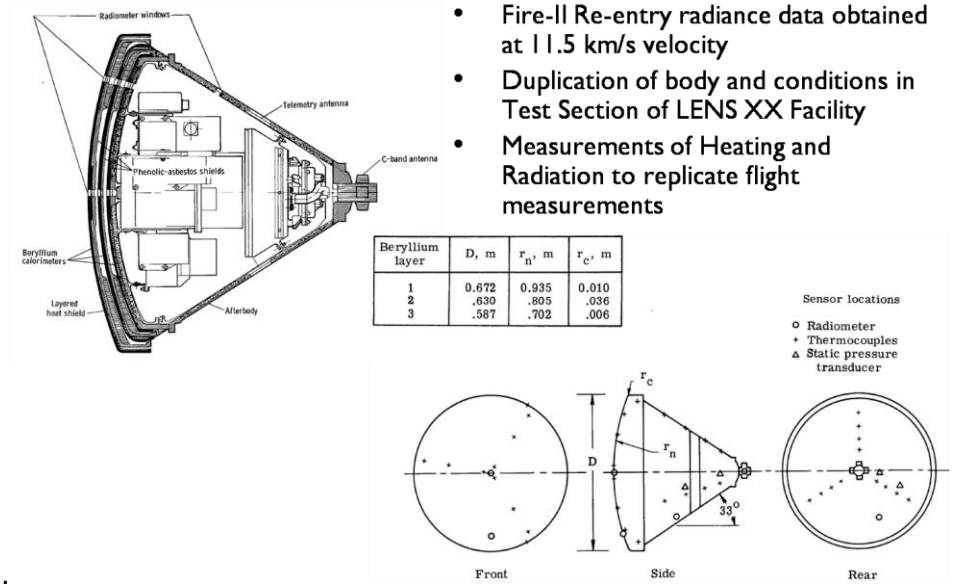

Figure 9: Heat Transfer Measurements to be Made in the LENS XX Tunnel at Duplicated Flight Conditions on Fire II Configuration

In the studies to measure electron density in ionized flows, we would replicate the RAM-C blunted cone configuration shown in Figure 10 and install surface and flowfield instrumentation similar to that used in the flight test program. In addition to obtaining electron density measurements with the Langmuir probe rake shown in Figure 11, we would plan to obtain measurements with antennas mounted in the surface of the model. If possible we would replicate the support system and instrumentation used in the flight tests shown in Figure 12.

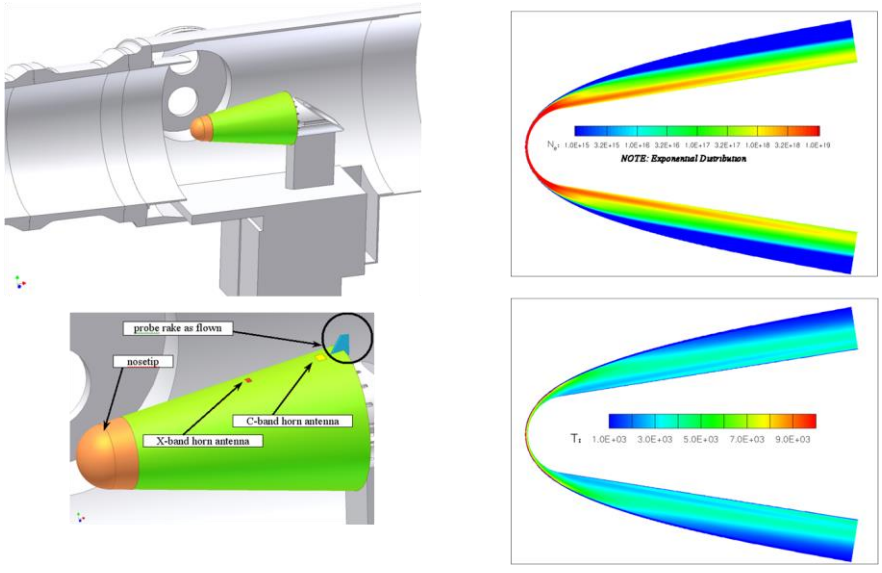

Figure 10: Duplication of Ram-C Flight Experiment in LENS XX Expansion Tunnel

Rake of Langmuir Probes

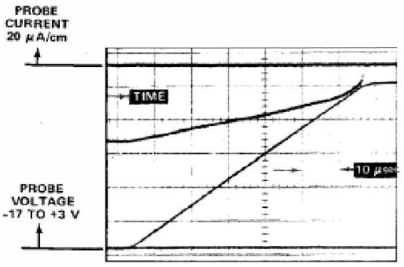

Typical Langmuir Probe Trace

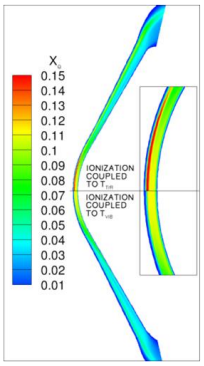

- Electron Temperature coupling is critical to electron formation rates.
- Direct measurements of electron temperature are desirable to validate numerical codes.

Figure 11: Instrumentation to Measure Electron Density and Temperature in Ionized Flows

.

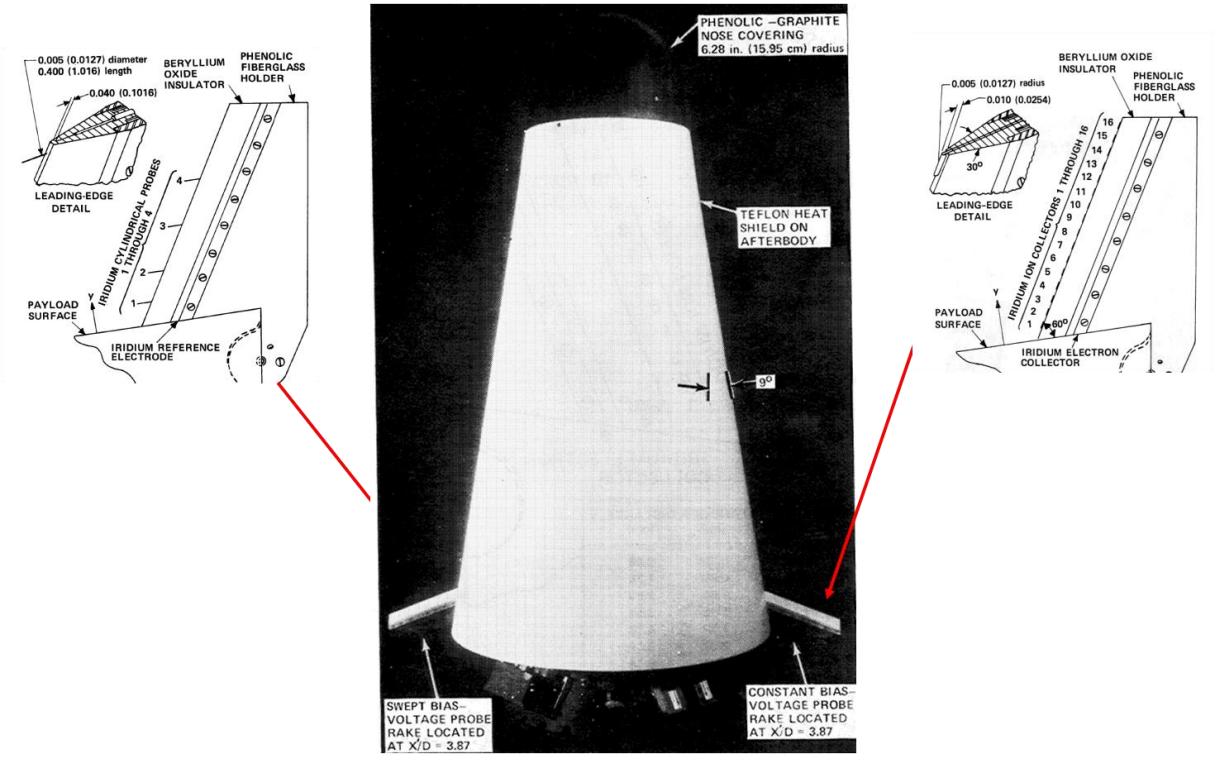

Figure 12: Ram-B/C Flight Experiments

3.0 SHROUD AND STAGE SEPARATION STUDIES IN LENS II

A number of studies have been performed in the LENS II shock tunnel to examine the separation of shrouds protecting the nosecone and engine inlets as they are boosted to hypersonic conditions in the atmosphere. These tests involved modifications to the test section to ensure that it could not be damaged or penetrated after the shroud had been released from the vehicle. We also constructed devices which were placed downstream to "catch" the flying objects to prevent them from accelerating to high speed and potentially causing severe damage to the back of the test section. Two full-scale models of the shrouds protecting the seekerhead for an Army interceptor and the inlets to the HyFly vehicle are shown in Figure 13a and b respectively. Shown in these photographs and Figure 14 are the stainless steel mats and catcher system designed to prevent damage to the facility.

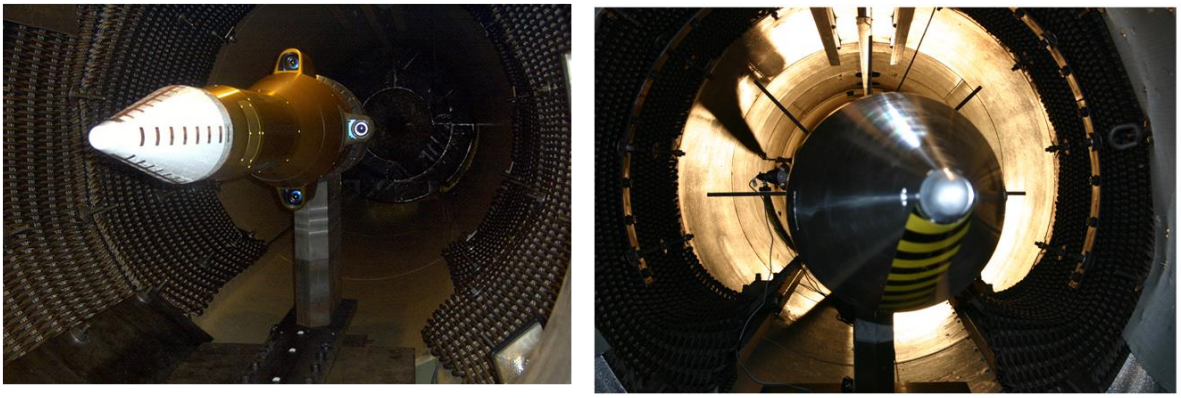

(a) Shroud for Army Interceptor

(b) Shroud Protecting Engine Inlets on HyFly Vehicle

Figure 13: Photograph of the Shroud Installation on the US Army's Interceptor Seekerhead and the HyFly Nosetip/Inlet Prior to Flight Duplication Testing

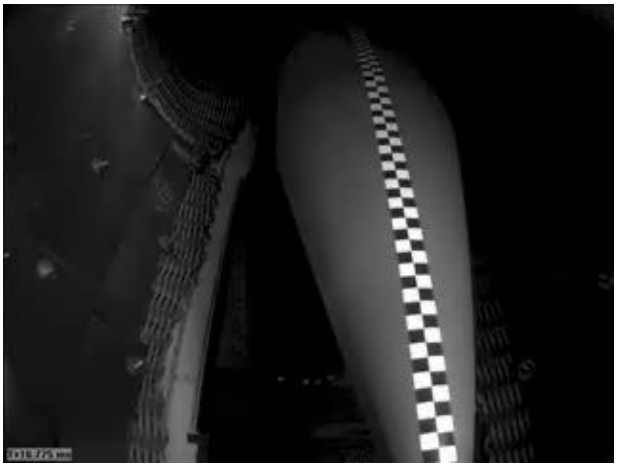

Figure 14: Cover Ejection

Comparison between the movement of the interceptor shrouds in the LENS II tests and numerical predictions performed with a unsteady Navier-Stokes code is shown in Figure 15. It shows that while the timing of the shroud removal differed slightly, the overall shock shapes were replicated with the exception of some unsteady shock phenomena which occurred near the end of the separation process. The unsteady heat transfer and pressure loading on the seekerhead window proved to be of significant interest with peak pressure loading over ten times those measured on the uncovered window configuration (Figure 16). These peak pressure and heat transfer levels which occurred in a region of shock wave/boundary layer interactions were not well predicted by computations.

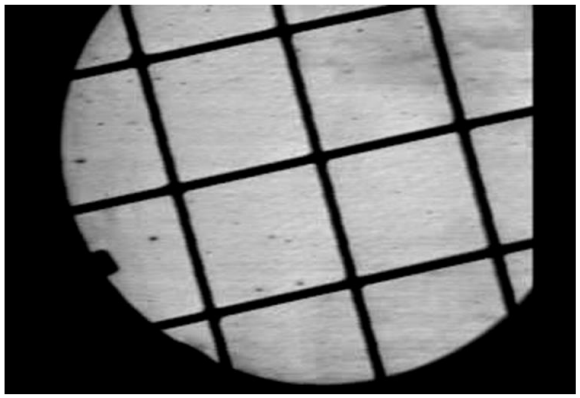

(a) High-Speed Video of Shroud Separation

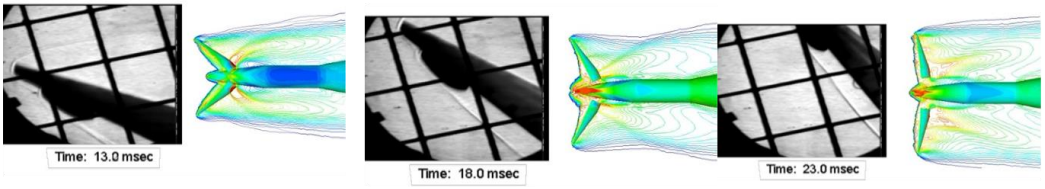

(b) Comparison between Ground Test Measurements and Numerical Computations

Figure 15: High-Speed Video Records during Shroud Separation and Comparison between Ground Tests and CRAFT Numerical Predictions

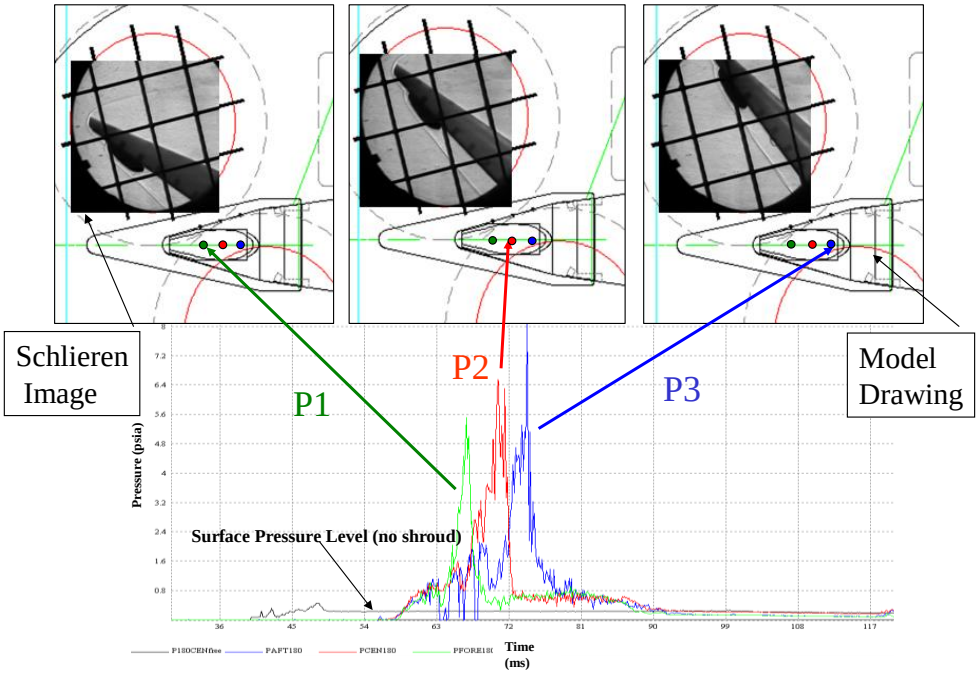

.

Figure 16: Unsteady Loading of Seekerhead Windows During Shroud Deployment

LENS II was also used in a "critical path" test to demonstrate that a new design for the HyFly shroud would work effectively in flight. Prior to these tests, both sled and flight tests were conducted with unsatisfactory results. Extensive preparations were made for this test, including a catcher system (see Figure 17a) to restrain the shrouds and prevent damage to the tunnel after they were ejected. Multi-view high-speed cameras (Figure 17b) were positioned to track the motion of the restrained and free motion of the shrouds as they separated. Measurements were also made to determine the forces on the shroud using an umbilical cord system which was severed after the shrouds had been released.

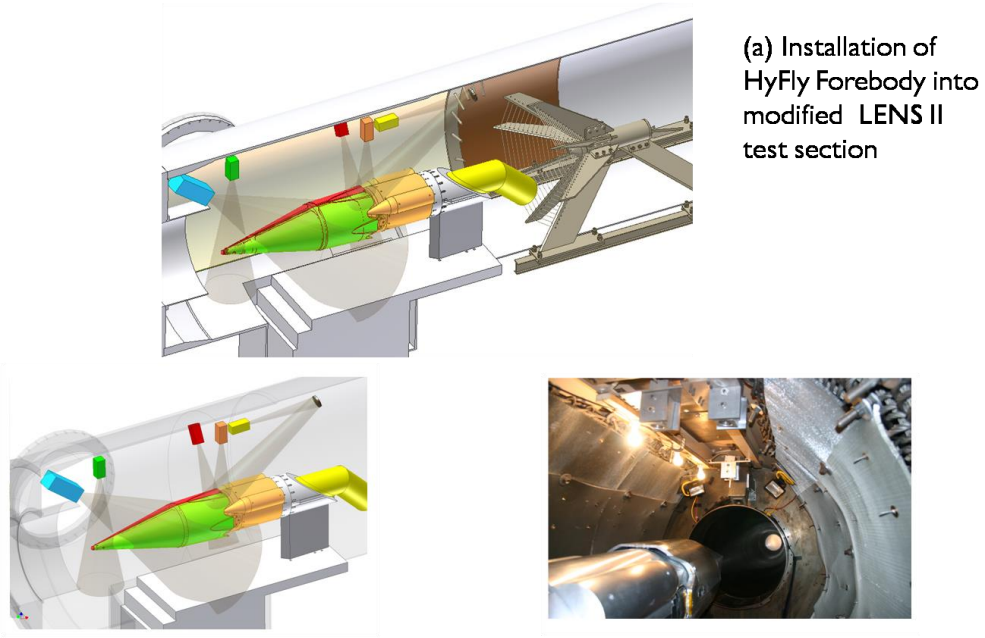

Figure 17: Installation of Full-Scale HyFly Shroud over Forebody of HyFly Dual Combustion Scramjet Engine

We used extensive CFD simulations in the design of this program, first to optimally position the full-scale test vehicle in the test section (see Figure 18), and then accurately establish the pressure under the shroud to match its flight value (Figure 18). The ground test to demonstrate the release of the shroud was successfully conducted and in subsequent flight tests, the shroud was ejected without incident.

"Free flight" stage separation tests have also been conducted in the LENS II facility. An example of this was a prototype for a rocket-launched penetrator where the penetrator was drag released from the rocket system, as illustrated in Figure 19. To accomplish these tests, the model was initially supported at its base from a sting system that could be rapidly withdrawn into the side of the tunnel. Key problems here were to release the model without significantly disturbing its attitude and withdraw the sting system so that the aerodynamics in the base region of the vehicle would not introduce extraneous behavior. As shown in Figure 19, the sting was actuated by a pneumatic cylinder which allowed us to withdraw the base support in a matter of milliseconds. At this time the vehicle was in "free flight" and a drag separation of the penetrator from the missile was successfully demonstrated.

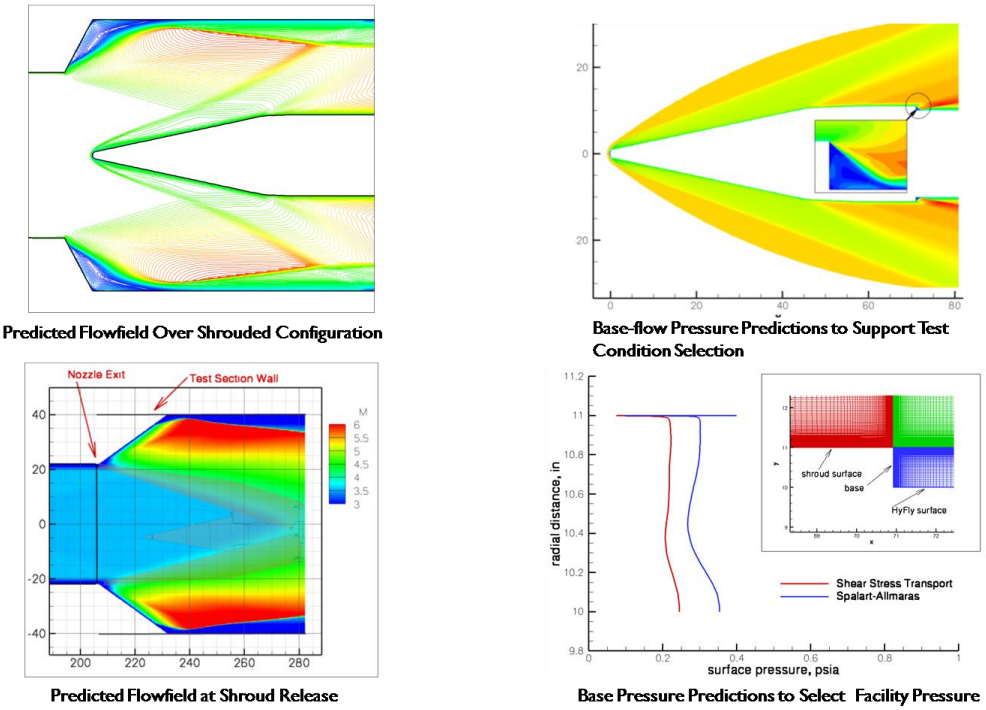

Figure 18: Computational Simulations Supporting Test Condition Selection

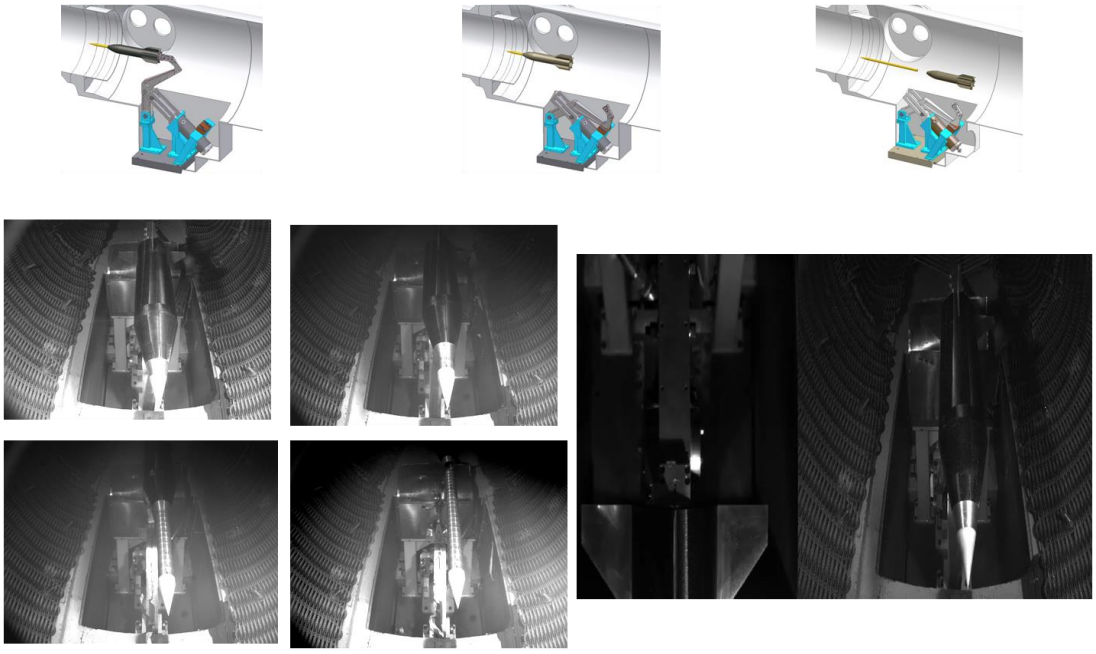

Figure 19: Model Release System and Video Sequence of the Drag Separation of the Penetrator from the Rocket Launcher

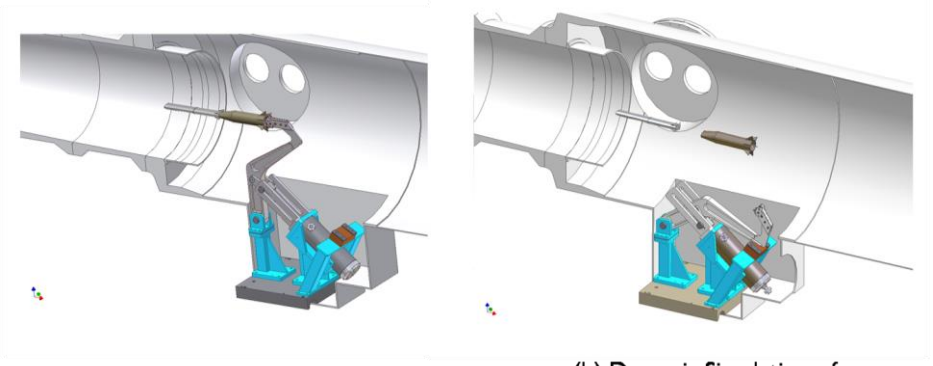

(a) Model Support System in Position to Achieve Steady Flow over the Vehicle

(b) Dynamic Simulation of Separation of Scramjet Engine from Booster

Figure 20: Scaling Studies of Rocket-Launched Scramjet Engine

Our main interest in developing this system was its potential use in studying stage separation of a rocket-launched scramjet engine where a system similar to that shown in Figure 20 will be employed.

4.0 FOAM AND ICE DEBRIS STUDIED FOR THE NASA SHUTTLE RETURN-TO-FLIGHT PROGRAM IN LENS II

One of the critical activities during the "return to flight" program of the shuttle was associated with validating the prediction techniques used to describe the trajectory of the foam as it was released from the surface of the main tank. Recall that the damage to the leading edge of the Orbiter wing was caused by an impact from frozen water-laden foam. In these tests, we ejected both foam divots and ice debris from the surface of a flat plate (see Figure 21) with a pneumatic plunger designed to accurately control the injection velocity. A vertical plate mounted perpendicular to the divot release system allowed us to accurately track the movement of the foam after it was released from the surface. In addition to tracking the toppling trajectory of a foam or ice divot, a key issue in these tests was to determine whether the divot remained intact during the interaction with the flow. Examples of situations where the divot remains intact and breaks up are shown in Figure 22(1) and 22(2).

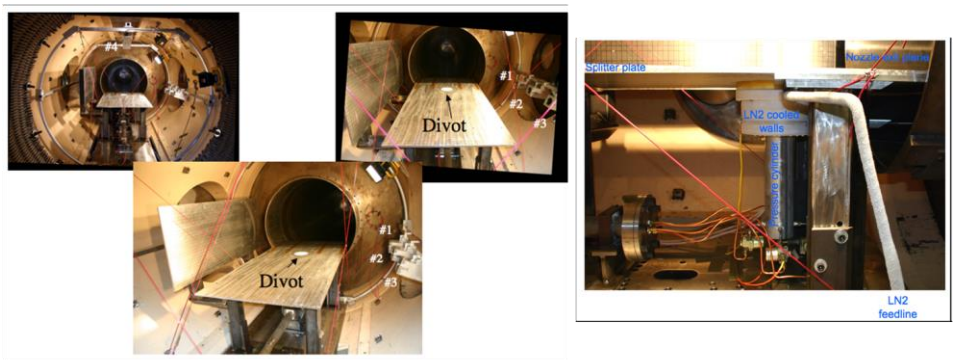

Installation of divot release system and camera installation in LENS II tunnel

Refrigerated hardware for divot/ice debris release

Figure 21: LENS II Tunnel Configured for Free Flight Studies of Foam Divots and Ice Divots

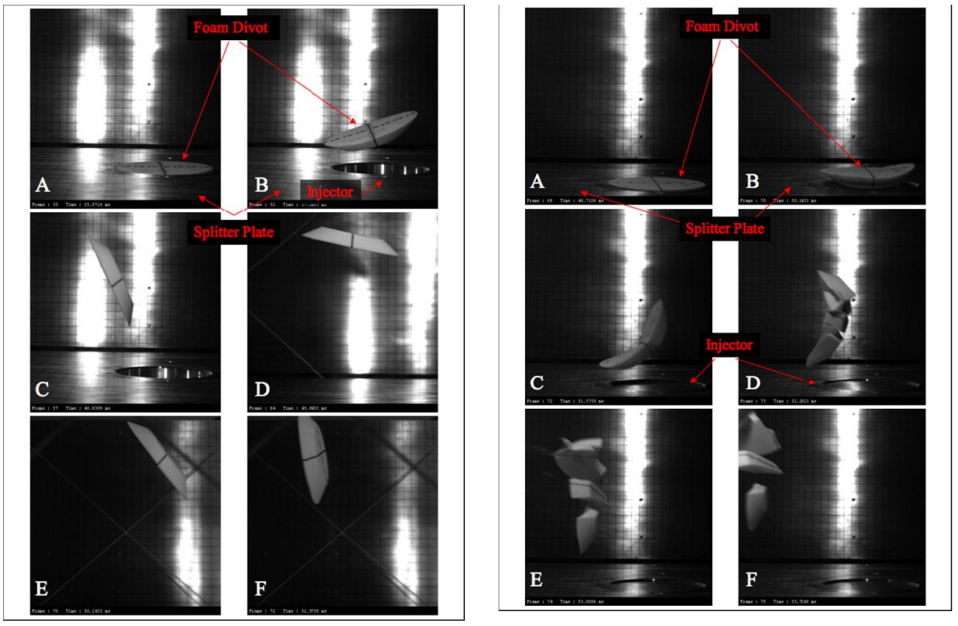

(1) Test Article Remains Intact (2) Test Article Breaks Up during Initial Flight

Figure 22: High-Speed Video Sequence of Trajectory of Divot where Test Article Remains Intact (1) and for Test Article Breakup (2)

5.0 FUNDAMENTAL STUDIES OF UNSTEADY FLOW PHENOMENA ASSOCIATED WITH STARTING DOOR AND MODE SWITCHING FOR RAMJET AND SCRAMJET ENGINES

In the past 10 years, a number of studies have been conducted to examine the performance of scramjet engines designed to fly at Mach numbers between 6 and 12. During these studies, we examined a number of key issues associated with inlet performance, shock interaction phenomena, flameholding and ignition, and mixing and combustion as outlined in Figure 23. Tests have been conducted in the LENS I and II tunnels to examine the performance of the NASP combustor, X-43 and HyTech flowpaths, full-scale HyFly, HyCAUSE and X-51 vehicles, and the DARPA "inward turning" ASET engine. These tests were conducted at the duplicated velocity/altitude conditions shown in Figure 24 with full-scale test articles.

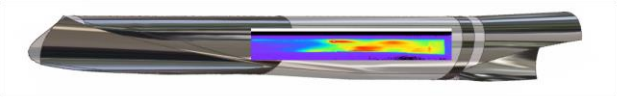

- Transition and tripping on inlet, isolator and combustor performance
- The effects of shock/boundary layer interactions on the inlet sidewalls, isolator, and combustor
- The effects of shock interaction and step and cavity flows on mixing
- Performance of auto- and forced- ignition systems and flameholding
- The mixing and combustion of the fuel in a compressible supersonic flow

Figure 23: Key Fluid-dynamic/Aerothermodynamic Problems which must be Understood and Predicted to Advance Scramjet Technology

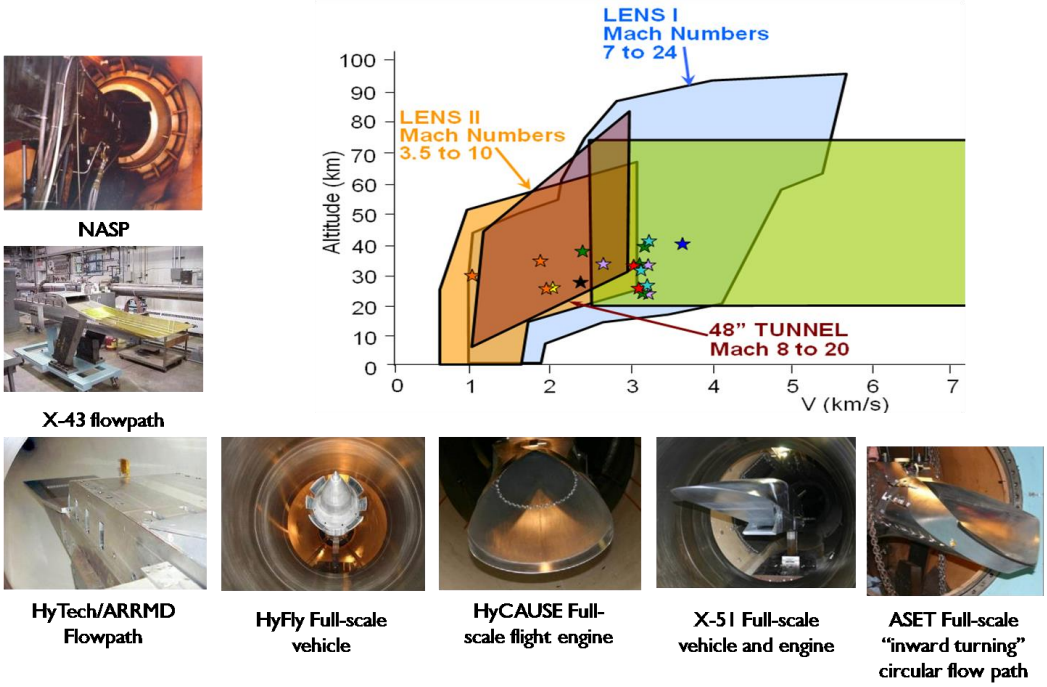

Figure 24: Background Experience in Scramjet Phenomenology and Testing [Full-Scale Engines at Duplicated Flight Conditions]

Fundamental studies have also been conducted in support of these programs to investigate shock/shock interaction heating, boundary layer transition and tripping on inlets, shock interaction phenomena with film and transpiration-cooled surfaces, attachment line transition, and re-laminarization in highly expanding flows. Models used in these tests are shown in Figure 25.

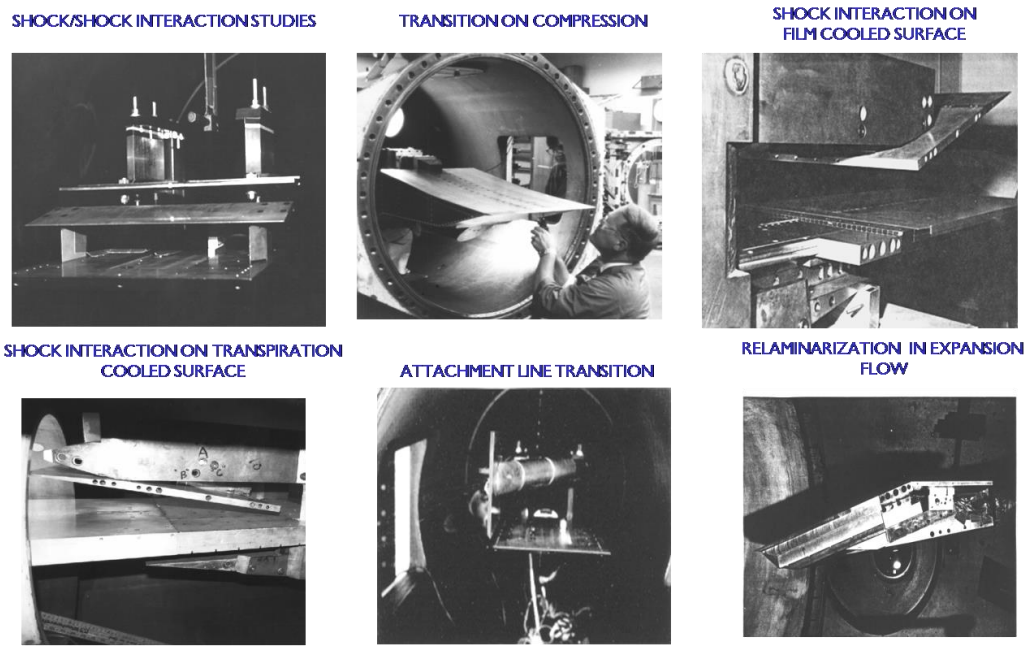

Figure 25: Studies of Fundamental Flow Phenomena for CFD Prediction/Validation for NASP

For highly contracted inlets such as those employed in the design of the HyCAUSE configuration it is necessary to employ starting door devices to obtain supersonic flow through the engine. A number of different concepts have been suggested as illustrated in Figure 26. For a starting device of the HyCAUSE engine, we selected the hinged door configuration shown in Figure 26(d). The testing to develop the starting door for the HyCAUSE engine was conducted in the LENS I facility at a Mach 8 freestream condition. This engine is shown installed in the LENS I test facility in Figure 27.

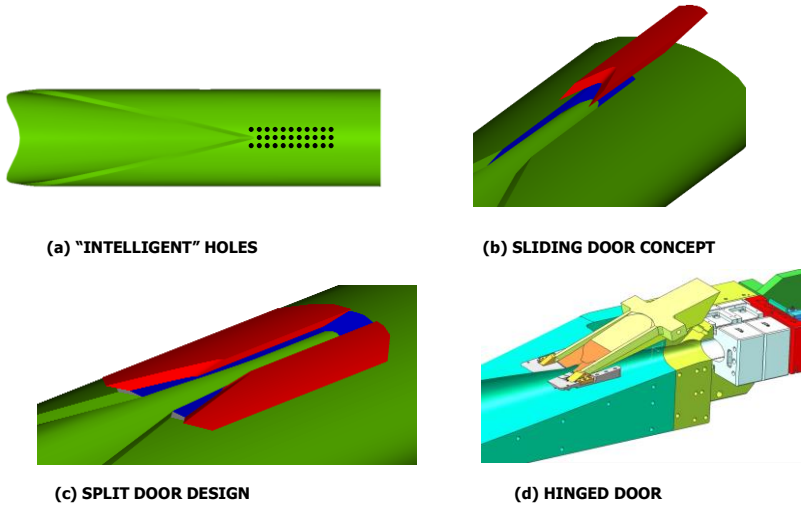

Figure 26: Concepts Studied for Starting Door Devices for "Inward Turning" Scramjet Inlets

Figure 27: Full-Scale Flight Test Configuration Installed in LENS I Tunnel for Mach 8 Studies

A number of different configurations were examined during this development program; two of which are shown in Figure 28(a). In our studies the position of the door hinge proved to be of critical importance as it influenced the shock interaction phenomena just inside the inlet. The selection of the final configuration was made through a combination of experiment and computation with the DPLR code (Figure 28(c)). In order to ensure that the flow was unstarted during the initial phase of the tests, we installed a slide valve in the isolator section of the engine as shown in Figure 28(b), which, once the flow was fully established over the engine, was opened to establish a well-defined unstarted flow through the engine.

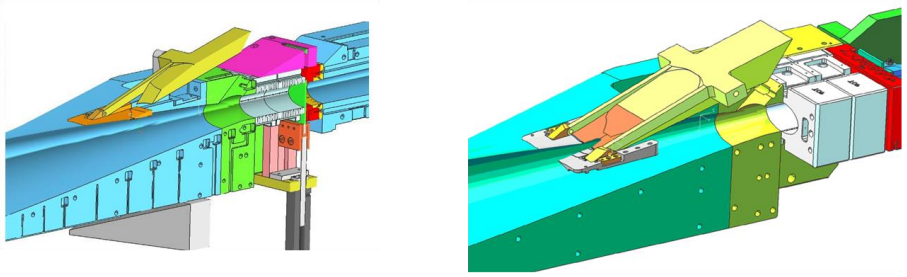

(a) The Two Inlet Door Configurations Studied during Development Testing

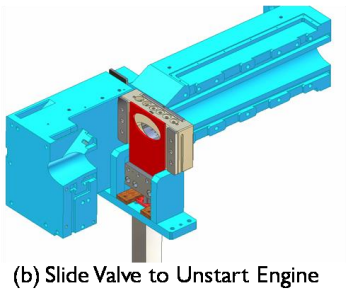

(b) Slide Valve to Unstart Engine

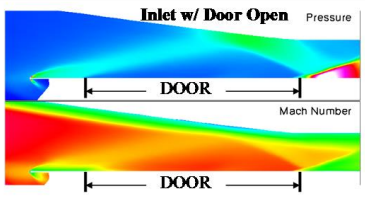

(c) Computer Simulation to Assess Shock Interaction Phenomena

Figure 28: Starting Door Configurations Studied During HyCAUSE Development Program

Shown in Figures 29 and 30 are examples of the starting process with a starting door design which resulted in an unsuccessful start (Figure 29) and one where the door was redesigned and the flow was successfully started (Figure 30). As mentioned earlier, a key issue was the shock interaction induced by

the inlet door, which in the case of the design shown in Figure 29 produced a separated region that enveloped the entire inlet. By eliminating the strong interaction in the inlet through the redesign of the door, as shown in Figure 30, we achieved a successful starting process through the engine as illustrated in the accompanying pressure traces.

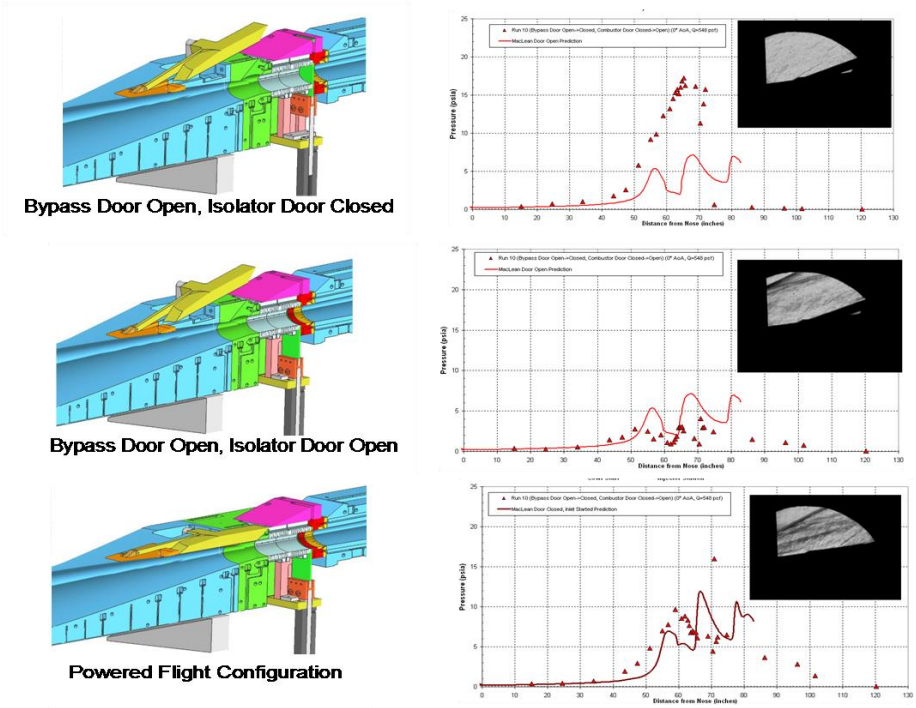

Figure 29: Measurements during the Investigation with the Unsuccessful Inlet Starting Door Configuration

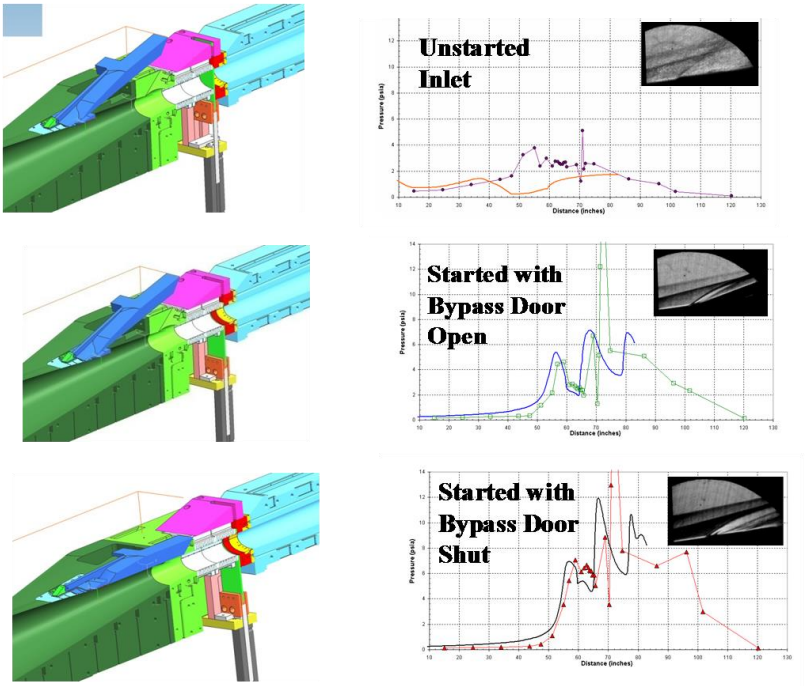

Figure 30: Measurements during the Investigation with the Successful Inlet Starting Door Configuration

Additional time history records shown in Figure 31 further illustrate the time sequences involved in the starting process. The pressure records from gages installed in front and behind the isolator door demonstrate that when we close the bypass door, we successfully start the engine for the final geometry of the starting door.

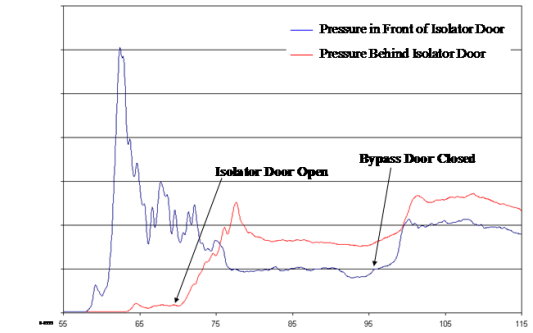

(a) Time History of Pressure Measurements ahead and behind the Inlet Isolation Gate Valve during Successful Engine Starting

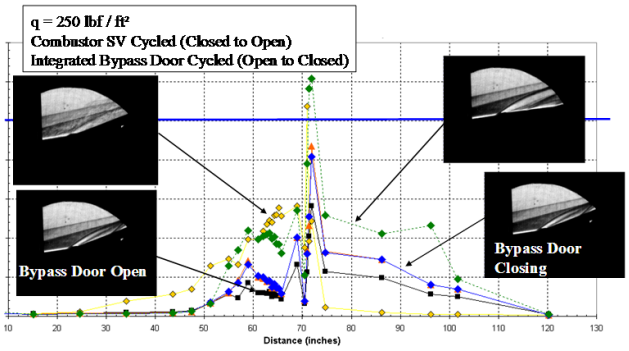

(b) Pressure Distributions through the Engine during Successful Engine Inlet Starting

Figure 31: Time History Pressure Records during Successful Engine Starting

An experimental program was conducted in conjunction with an AFOSR MURI activity to develop numerical tools to predict the unsteady flow phenomena during mode switching, which included both the starting door and the turbine-to-ramjet mode transition phenomena as illustrated in Figure 32. For turbine-based combined cycle engines, a major issue is switching between the low-speed operation with a turbine and ramjet operation. This operation requires a sequential closing of the turbine inlet and opening the ramjet inlet in a manner to maintain a consistent thrust on the engine. In studies in the LENS II facility, we employed a full-scale flowpath of the size used in the X-51 vehicle, which was modified to incorporate inlet doors in front of the turbine and ramjet profiles. In these studies we examined the starting process of the engine for two configurations of the turbine starting door inlet, an outward opening door (Figure 33(a)) and inward opening door (Figure 33(b)).

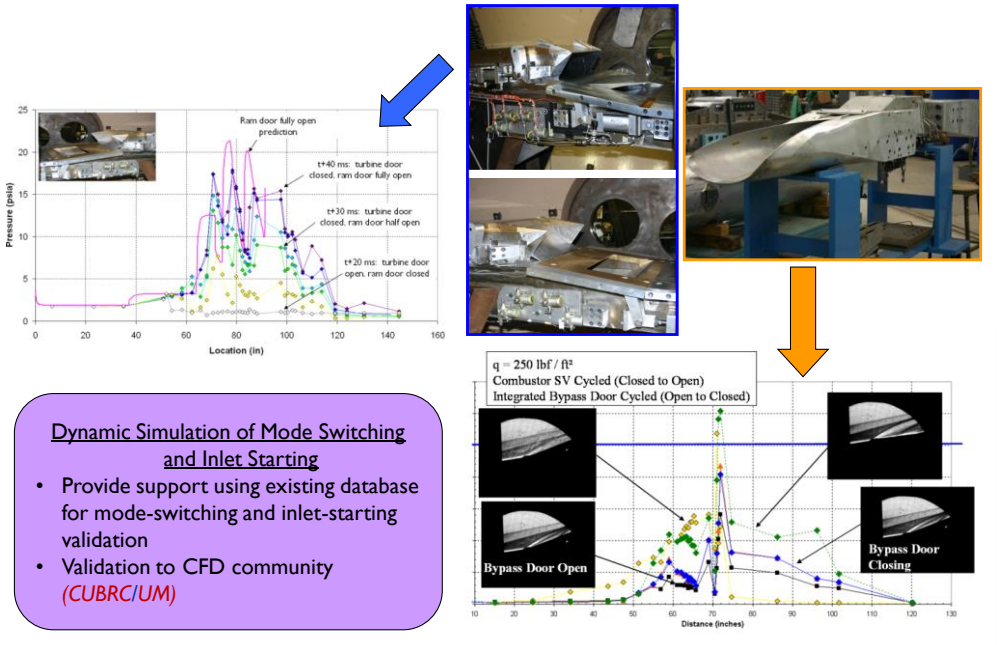

Figure 32: Numerical Simulation of the Unsteady Flow Dynamics during Mode Switching using CUBRC Measurements from MURI to Validate CFD Tools [UM and CUBRC]

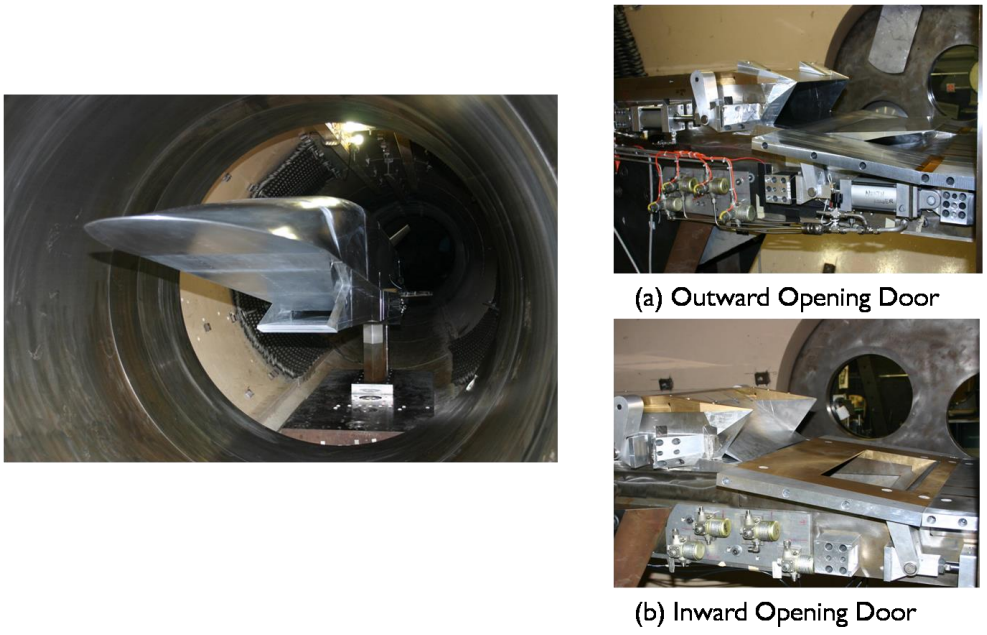

Figure 33: Studies of Mode Switching with a Full-Scale Flow Path Typical of the Size Used in the X-51 Vehicle

Photographs and schematic diagrams of the inward- and outward-opening turbine door configurations studied in this program are shown in Figure 34.

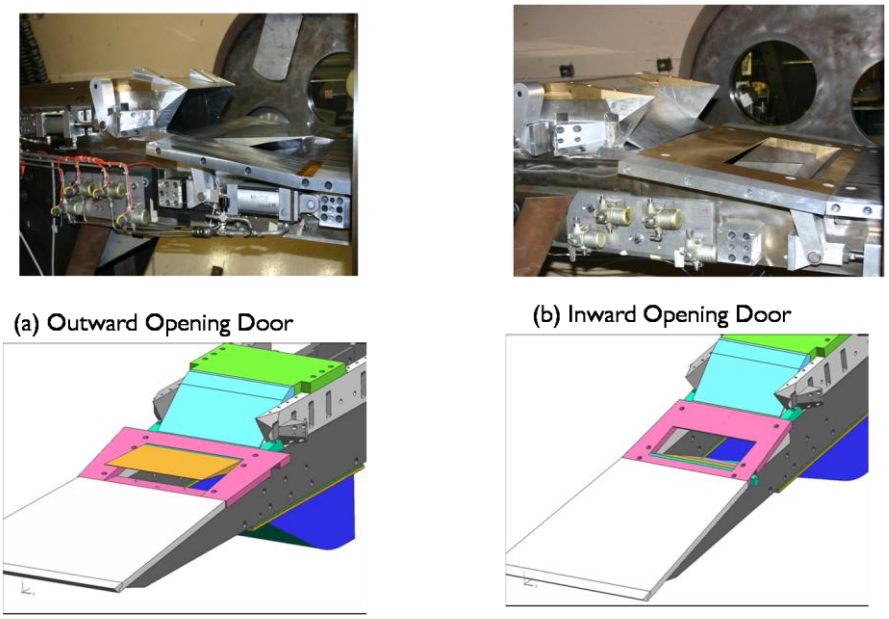

Figure 34: Installation of Full-Scale Engine with Outward Closing and Inward Closing Turbine Inlets in LENS II Tunnel for Mode Switching Studies

During this program, a significant effort was expended in designing a turbine door configuration which started successfully. Here the key problem was associated with shock-induced separated flows which choked the turbine inlet and resulted in inlet unstart for a poorly designed inlet configuration. Again, both experiment and computations with the DPLR code were employed to generate a configuration which started successfully. Figure 35 shows unsuccessful and successful designs for the inlet, the difference being on the details of the turning angles on the door and inside the inlet to prevent shock-induced flow separation. Figure 36 shows the time history in the inlet duct for the final inlet door configuration which demonstrates a fully developed uniform flow before the turbine door is closed. Pressure records from the flow inside the ramjet section of the engine shown in Figures 37 and 38 demonstrate that for the final door designs, the flow through the ramjet section of the engine can be started smoothly.

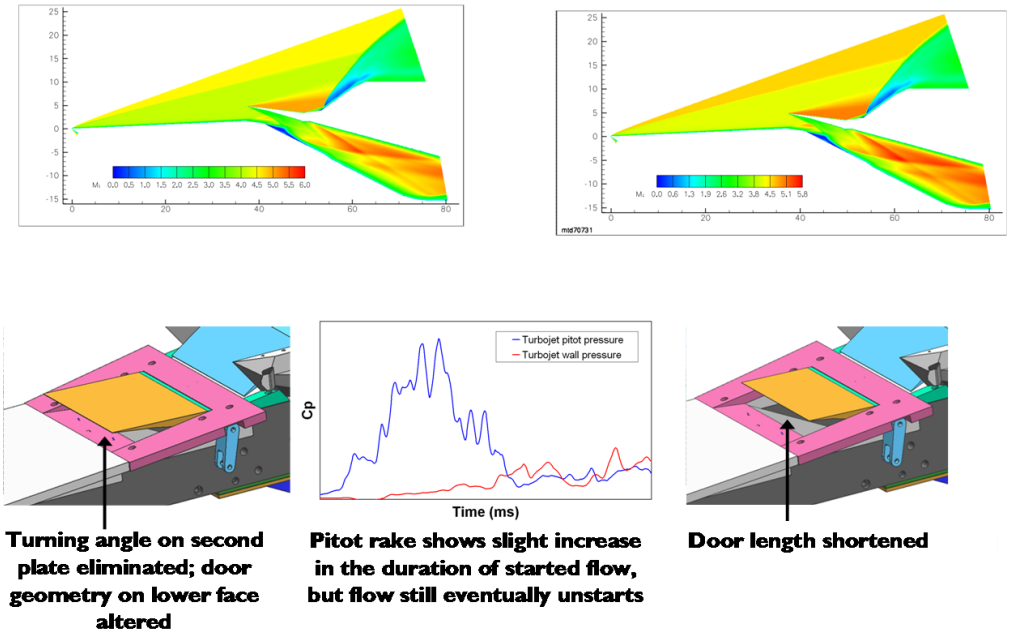

Figure 35: Development of Outward Opening Door Configuration to Achieve Successful Starting

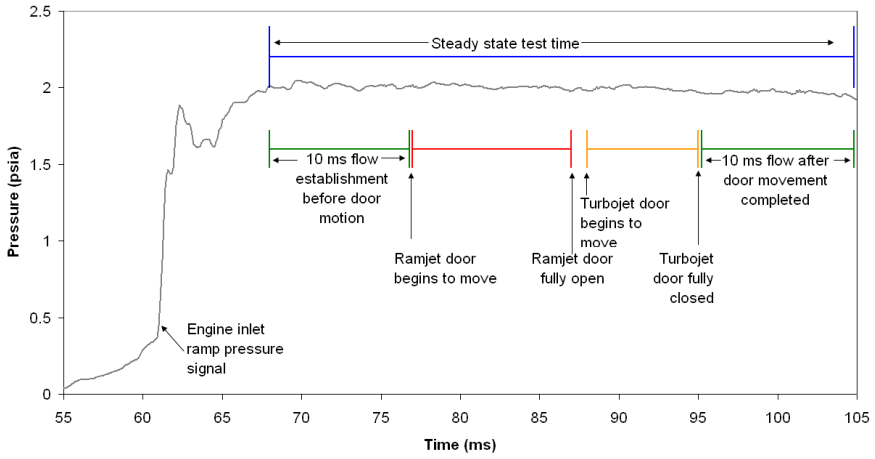

Figure 36: Time History of Tunnel Pressure showing Sequence of Door Operation

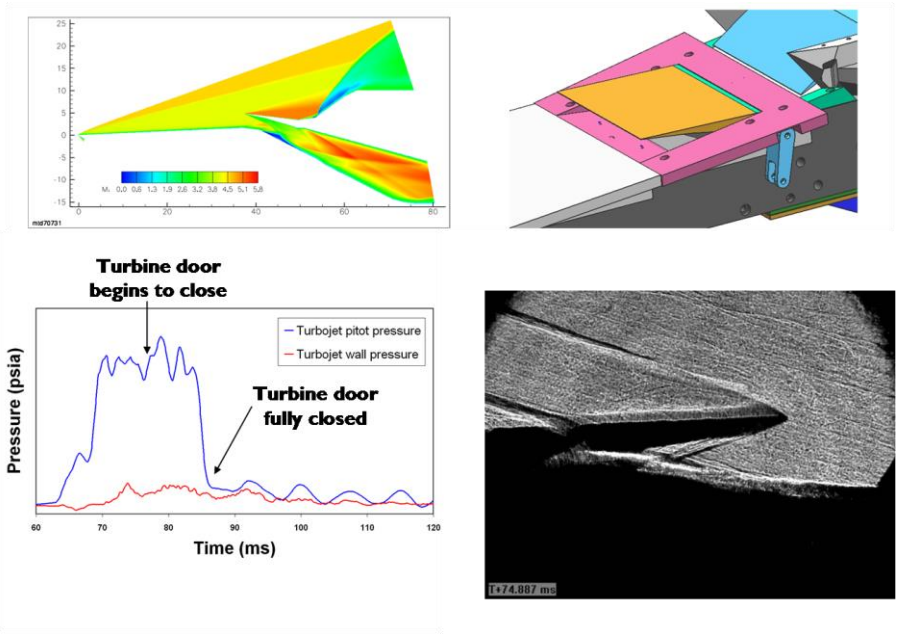

Figure 37: Final Door and Inlet Geometry Configuration Developed for Turbine Inlet Door

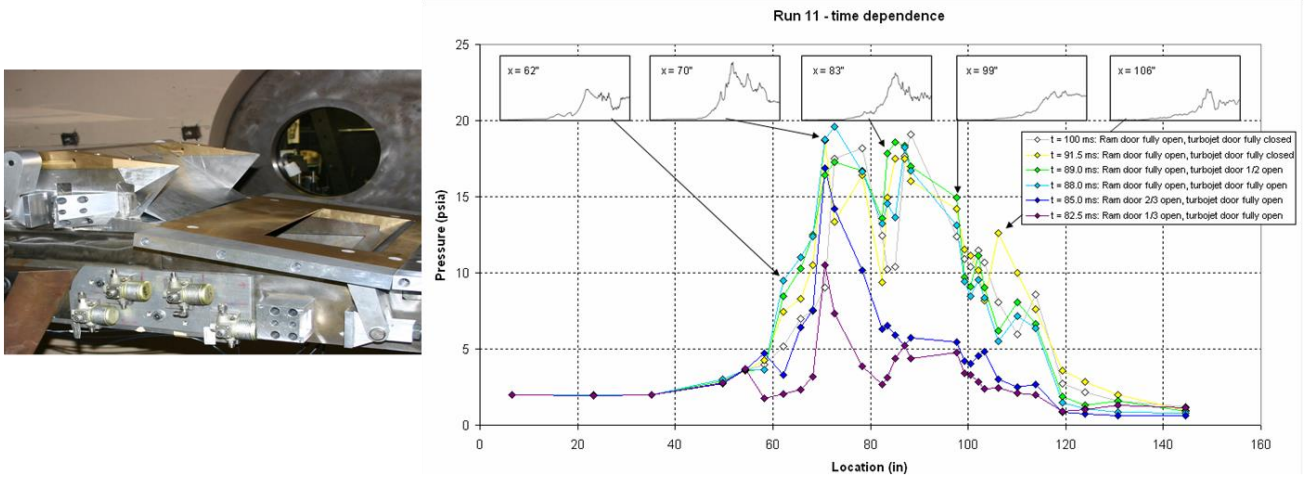

Figure 38: Pressure Histories during Mode Switching from Turbine to Ramjet Operation with Inward Opening Turbine Door

We have obtained direct measurements of thrust and drag on a full-scale scramjet engine suspended in the LENS I tunnel by using an accelerometer-based balance system. Figure 49 shows a schematic diagram of a full-scale ASET engine softly suspended from a framework which is mounted independently from the tunnel through an inertial mass system. This system is designed so that for the 20 ms run period, the model is freely flying and the drag and thrust forces can be determined directly from a three-component accelerometer balance constructed in the engine. For these studies, the fueling systems and the 58-channel data recording systems were installed into the engine module. The engine module is supported from four sets of springs mounted on the subframe which is itself isolated from the inertial block through isomode pads (see Figure 39). A centerbody is used to terminate the flow once

the useful test time is over, and the model is prevented from moving further by a mechanical snubbing system also shown in Figure 39. A model suspended from the LENS I tunnel is shown in Figure 40, together with a schematic diagram showing the installation of the fuel and data systems.

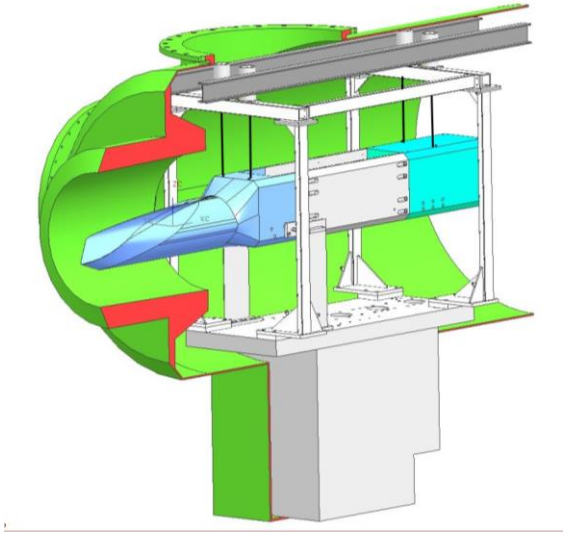

Figure 39: Direct Measurements of Thrust and Drag on Scramjet Engine Using Accelerometer Balance System

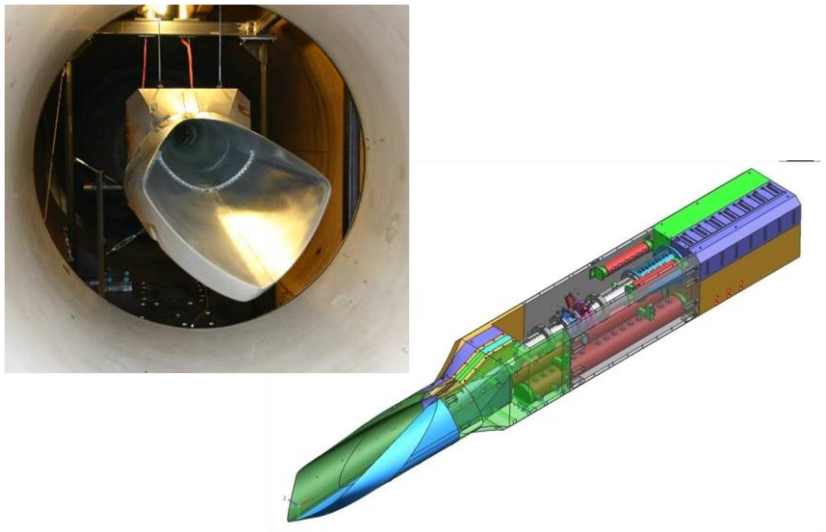

Figure 40: ASET Engine Suspended in LENS I for "Free-flight" Measurements of Thrust and Drag

In a complementary series of tests, we obtained direct measurements of the thrust and drag on individual components of this engine by mounting each segment of the engine separately on an inertial block through flextures and strain gage force measurements modules. A schematic diagram of the installation of the assembly of the injector, combustor and nozzle sections of the engine are shown in Figure 41. The measurements of thrust and drag on each component were obtained with five-component force and accelerometer balances assembled as shown in Figure 41.

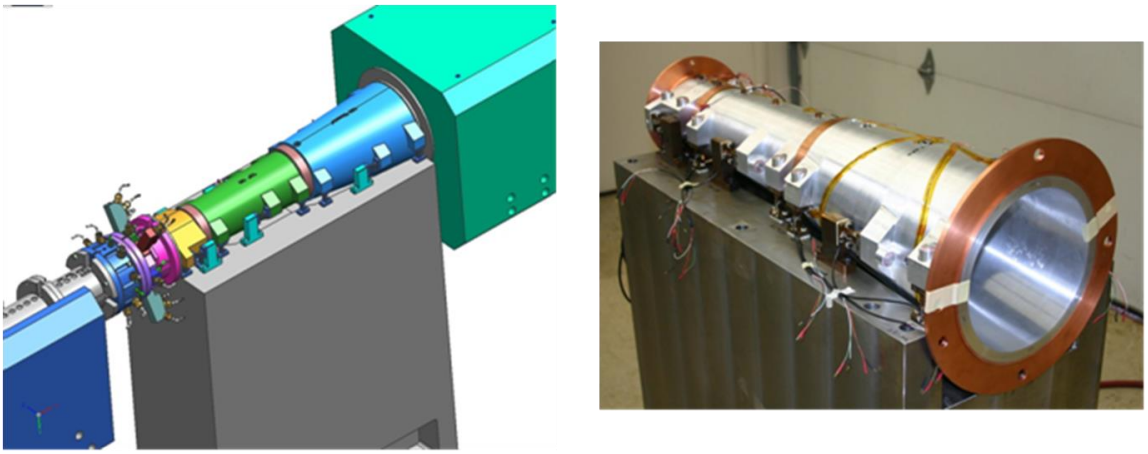

Figure 41: Three Thrust/Drag Balance Modules for ASET Combustor

Measurements made in this series were used to improve the engineering models to calculate scramjet performance and in particular develop Reynolds analogy relationships to predict skin friction from the measurements of heat transfer.

Also during the MURI program, we constructed and obtained measurements in a combustion duct to examine key phenomena associated with the performance of scramjet engines. This combustion duct was designed to provide the well-defined flow environment against which to evaluate code predictions. The size and proportion of this duct was also similar to the HIFiRE 2 engine which is being developed to be used in the Australian HIFiRE 2 program. Figure 42 shows a schematic diagram of the combustion duct and key objectives to provide measurements with which to develop and evaluate numerical models of key importance to computing scramjet performance.

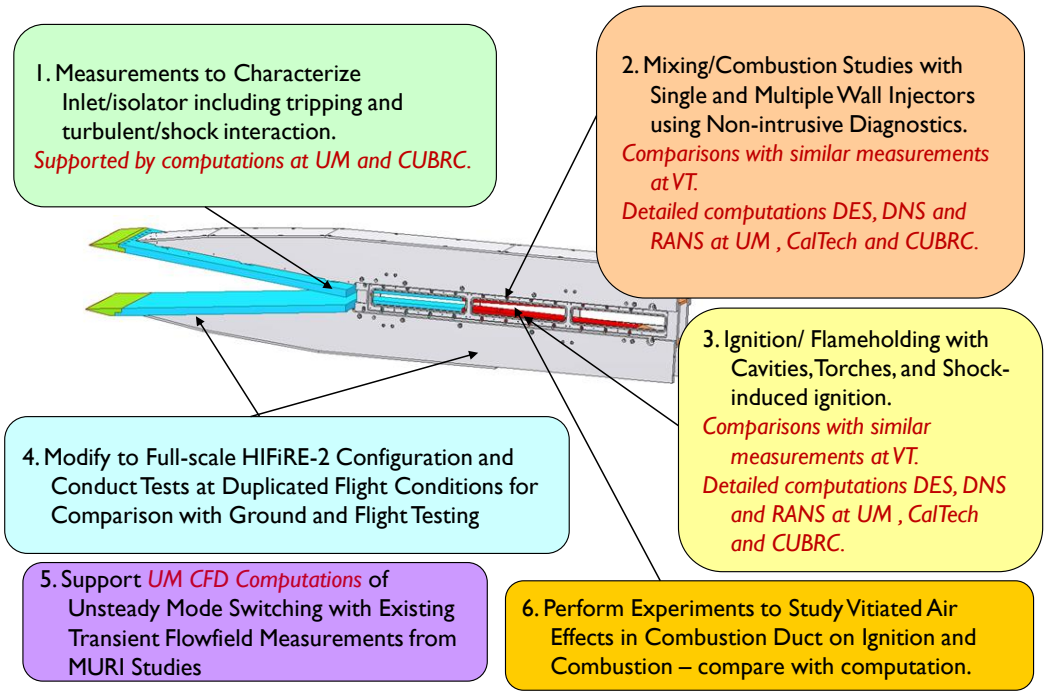

Figure 42: CUBRC Combustion Duct Constructed Under the MURI Program to Investigate Key Aerothermal Phenomena Associated with Scramjet Propulsion

Figure 43 shows a photograph of the scramjet duct and the installation of this system into the LENS I tunnel. A Schlieren photograph and a representative sample of the distribution of pressure and heat transfer through the duct for a mixing run is also shown in Figure 43. Comparisons between pressure measurements through the scramjet duct and calculations using the DPLR code are shown in Figure 44 for configuration A with a symmetric inlet. The agreement between prediction and experiment is remarkably good considering the complexity of this flow. Also shown in Figures 44, 45 and 46 are the objectives for fundamental studies to examine the ability of the current DES and RANS models to predict mixing and combustion, and ignition and flameholding in a simple two-dimensional combustion duct.

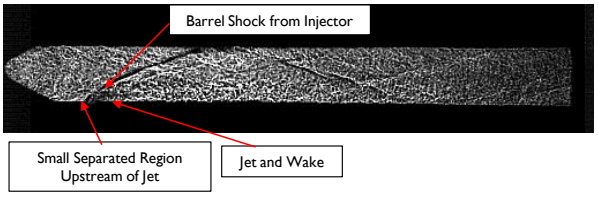

Schlieren Image of Mixing Run

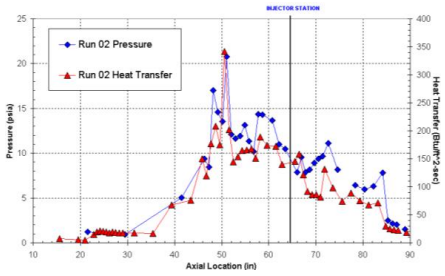

Surface Measurements from Mixing Run

Figure 43: Scramjet Duct Model and Results from MURI Test Program

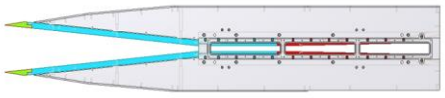

Config A. Duct Model with Symmetric Style Inlet

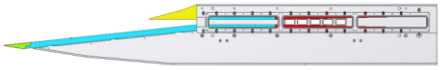

Config B. Duct Model with Cowl Style Inlets

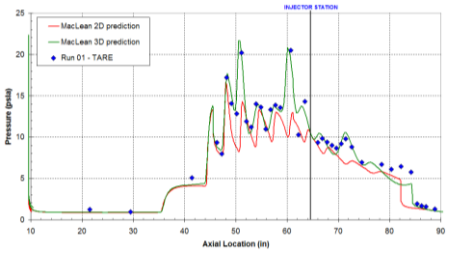

CFD and Experiment of Flowpath

Characterization of Inlet and Isolator Performance

- Key technical problems:
  - Tripping and turbulent radiated transition
  - Turbulent BL/Shock Interaction
- *Supported by computations at UM and CUBRC using both DES and RANS models.*

Test conditions duplicating flight from Mach 6 to 10

Surface Measurements

High frequency pressure and thin-film heat transfer

Skin friction

Flowfield Measurements

NO and OH PLIF measurements

H_2O Tomography

Infrared

Figure 44: Surface and Flowfield Characterization of Inlet and Isolator Performance

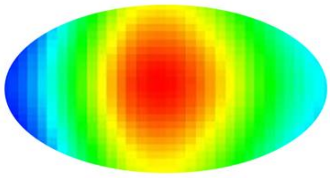

H_2O concentration

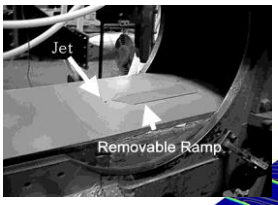

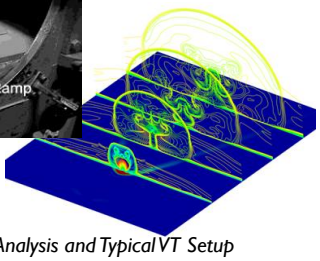

CFD Analysis and Typical VT Setup

Mixing and Combustion Studies

- "Simple" configurations in 2D duct model starting with 1 jet.
- Heavy emphasis on non-intrusive diagnostics (PLIF, TDLAS, CARS, etc) *(CUBRC/NASA).*
- Comparison of hot versus cold mixing flows to obtain comparisons with VT *(CUBRC/VT).*
- Comparisons with both DES and RANS CFD & assessment of turbulence model capabilities *(CUBRC/UM/CalTech).*

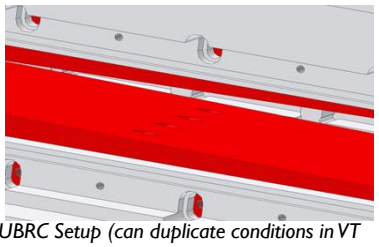

CUBRC Setup (can duplicate conditions in VT tunnel)

Figure 45: Fundamental Study of Mixing and Combustion and Supporting CFD Analysis

Plasma Torch

Conventional Cavity

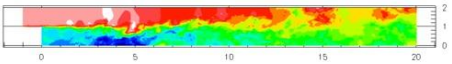

CalTech Step Cavity

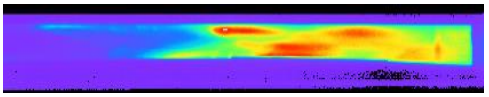

Shock Induced Ignition

Ignition and Flameholding Study

- Comparison of auto-ignition, shock-induced ignition, and forces ignition (H_2/O_2 and plasma/spark torches) (CUBRC/VT)
- Comparison of conventional and step cavity for flameholding (CUBRC/CalTech)
- CFD validation modeling (CUBRC/UM/CalTech)

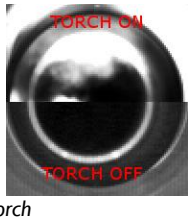

H_2/O_2 Torch

Figure 46: Study of Flameholding and Ignition Processes including Effect of Shock-induced Ignition

Figure 47 shows the modifications that could be made to our combustion duct to produce full-scale measurements at duplicated flight conditions on a full-scale version of the HIFiRE-2 configuration.

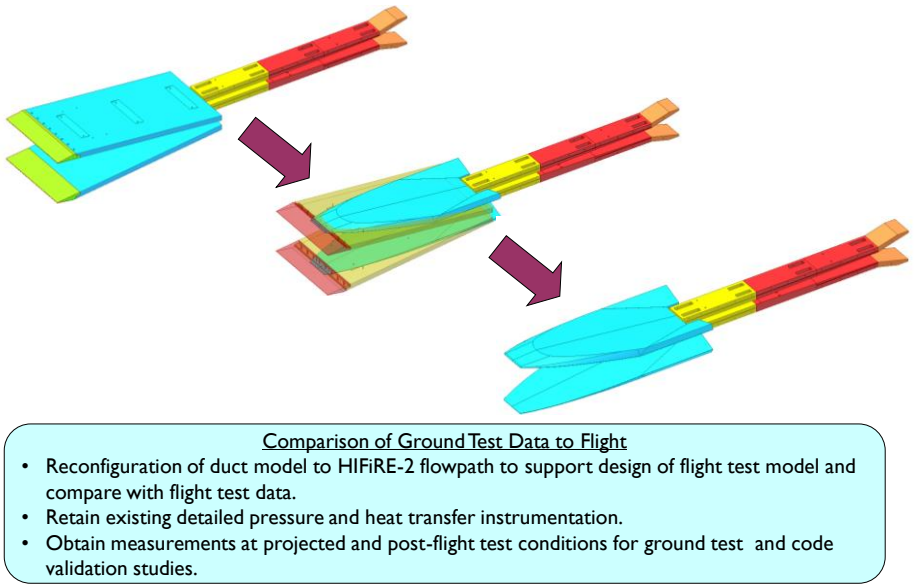

Figure 47: Modification of Scramjet Duct Model to Obtain Full-scale HIFiRE-2 Configuration – Supporting the HIFiRE Flight Test Program

Finally during the MURI program, we investigated the effects of vitiated air on the performance of a full-scale Mach 6 scramjet engine run with hydrogen and hydrocarbon fuels. For these studies, modifications depicted in Figure 48 were made to the driven section of the LENS II facility to introduce vitiants into the driven section of the tunnel to produce flow constituents in the freestream which were similar to those generated in a combustion-driven tunnel. We first demonstrated that we could replicate the vitiants in the freestream using laser diode and spectrographic analysis. Then, we compared the performance of the hydrogen- and hydrocarbon-fueled engine under vitiated and nonvitiated air conditions. These studies suggested that while the performance of hydrogen-fueled engine was not significantly affected by vitiation, this was not the case for the engine fed with hydrocarbon fuels. In the latter case, both fuel ignition and the final combustion pressure differed significantly between vitiated and nonvitiated flow environments.

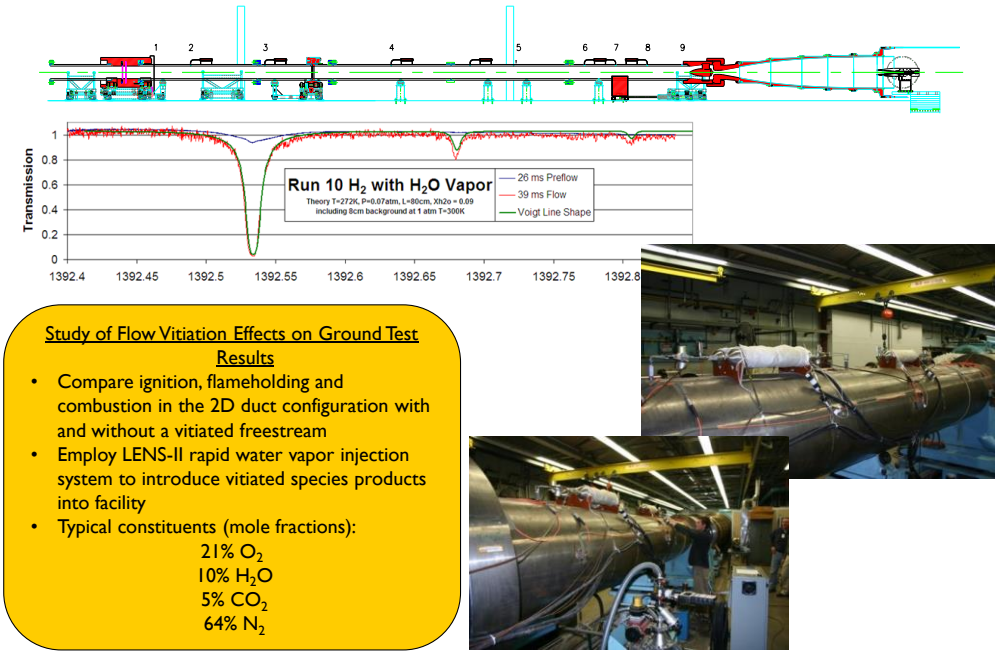

Figure 48: Experimental/Computational Study of Vitiated Air Effects for Hydrogen and Hydrocarbon Fuels

7.0 SUMMARY

During the past four years, a new ground test capability and innovative test techniques have been developed to investigate unsteady flow phenomena associated with "free flight" of multi-component vehicles. A high-speed valve, rapidly retracting sting, and capture systems have been developed to safely handle the large kinetic energies that can be generated in tests with free-flying objects in a hypersonic test environment. Mode switching studies associated with inlet=starting devices and transition from turbine to ramjet operation have been conducted with full-scale hardware at duplicated flight conditions for the Australian/American HyCAUSE Program and for a turbine/scramjet engine vehicle in a MURI Program for the U.S. Air Force.

BIBLIOGRAPHY

1. Holden, M.S. and Parker, R.A., "LENS Hypervelocity Tunnels and Application to Vehicle Testing at Duplicated Flight Conditions", Chapter 4, AIAA Publication ***Advanced Hypersonic Test Facilities***, Frank K. Lu, Editor, published September 2002.

2. Holden, M.S, and Wadhams, T.P., "A Database of Aerothermal Measurements in Hypersonic Flows in 'Building Block' Experiments for CFD Validation," AIAA 2003-1137, 41st Aerospace Sciences Meeting and Exhibit, Reno, NV, January 6-9, 2003

3. Holden, M. S., Harvey, J., MacLean, M., Wadhams, T., Walker, B.J., "Development & Application of New Ground Test Capability to Conduct Full-Scale Shroud/Stage Separation," AIAA 2005-0696, 43rd AIAA Aerospace Meeting and Exhibit, Reno, NV, January 10-13, 2005.

4. Holden, Michael S., "Aerothermal and Propulsion Ground Testing that Can Be Conducted to Increase Chances for Successful Hypervelocity Flight Experiments", the von Karman Institute, October, 2005, Brussels, Belgium. To be published in RTO Course "Flight Experiments for Hypersonic Vehicle Development."

5. Holden, Michael S., Wadhams, Timothy P., Smolinski, Gregory J., MacLean, Matthew G., Harvey, John and Walker, Bill J., "Experimental and Numerical Studies on Hypersonic Vehicle Performance in the LENS Shock and Expansion Tunnels," AIAA 2006-0125, 44th AIAA Aerospace Sciences Exhibit & Meeting, Reno, NV, January 8-12, 2006.

6. Smolinski, Gregory J., Wakeman, Thomas R., and Holden, Michael S. "Experimental Aerodynamic Transport Characterization of Space Shuttle Debris using Stereogrammatics," AIAA 2006-0721, 44th AIAA Aerospace Meeting & Exhibit, Reno, NV, January 9-12, 2006.

7. Parker, Ronald A., Wakeman, Thomas, MacLean, Matthew and Holden, Michael, "Nitric Oxide Concentration Measurements with a Quantum Cascade Laser in the LENS I Hypersonic Shock Tunnel Facility," AIAA 2006-926, 44th AIAA Aerospace Meeting & Exhibit, Reno, NV, January 9-12, 2006.

8. Holden, Michael S., Wadhams, Timothy P., MacLean, Matthew, Parker, Ronald A., "Experiments in Numerical Studies of Low Density and Real Gas Effects on Regions of Shock Wave/Boundary Layer Interaction in Hypervelocity Flows," Report No. A-06-U-006, June 2006

9. Holden, Michael S., Wadhams, Timothy P., MacLean, Matthew, Mundy, Erik and Parker, Ronald, "Experimental Studies in LENS I and LENS X to Evaluate Real Gas Effects on Hypervelocity Vehicle Performance," AIAA 2007-204, 45th Aerospace Meeting & Exhibit, Reno, NV, January 8-11, 2007.

10. Holden, Michael, Wadhams, Timothy, MacLean, Matthew, and Walker, Bill J., "Experimental Studies in Hypersonic Flows for Facility and Code Validation," AIAA 2007-1304, 45th Aerospace Meeting & Exhibit, Reno, NV, January 8-11, 2007.

11. Nompelis, I., Candler, G., Holden, M. and MacLean, M., "Investigation of Hypersonic Double Cone Flow Experiments at High Enthalpy in the LENS Facility," AIAA 2007-203, 45th Aerospace Meeting & Exhibit, Reno, NV, January 8-11, 2007.

12. Parker, Ronald, Wakeman, Thomas, MacLean, Matthew and Holden, Michael, "Measuring Nitric Oxide Freestream Velocity using Quantum Cascade Lasers at CUBRC," AIAA 2007-1329, 45th Aerospace Meeting & Exhibit, Reno, NV, January 8-11, 2007.

13. MacLean, M.; Mundy, E.; Wadhams, T.; Holden, M.; Johnson, H.; Candler, G. "Comparisons of Transition Prediction using PSE-Chem to Measurements for a Shock Tunnel Environment." AIAA Paper 2007-4490. 37th AIAA Fluid Dynamics Conference & Exhibit, Miami, FL: 25 - 28 June 2007

14. Wadhams, T.P., Mundy, E., MacLean, M.G., Holden, M.S., "Pre-Flight Ground Testing of the Full-Scale HIFiRE-1 Vehicle at Fully Duplicated Flight Conditions, Part II," AIAA 2008-0639, 46th AIAA Aerospace Sciences Meeting and Exhibit, Reno, NV, Jan. 7-10, 2008.

15. Holden, M.S., Smolinski, G.J., Mundy, E., MacLean, M., Wadhams, T.P., Walker, B.J., "Experimental Studies for Hypersonic Vehicle Design and Code Validation of the Unsteady Flow Characteristics associated with "Free Flight" Shroud and Stage Separation, and Mode Switching," AIAA 2008-0642, 46th AIAA Aerospace Sciences Meeting & Exhibit, Reno, NV, Jan 7-10, 2008.

16. Holden, Michael S., Wadhams, Timothy P., MacLean, Matthew, "Experimental Studies in the LENS Supersonic and Hypersonic Tunnels for Hypervelocity Vehicle Performance and Code Validation," AIAA 2008-2505, AIAA Meeting, Dayton, OH, April 28-30, 2008.

17. Holden, Michael S., Smolinski, Gregory J., Mundy, Erik, MacLean, Matthew and Wadhams, Timothy P., "Full-Scale Tests of Inlet Starting, Mode Switching and Component Separation at Fully Duplicated Flight Conditions," JANNAF-1022, 30th JANNAF Meeting, Boston, MA, May 12-16, 2008.

18. Smolinski, Gregory J., Holden, Michael S., Wakeman, Thomas, and MacLean, Matthew, "Full-Scale Free Flying HyFly Shroud Ejection Test at Fully Duplicated Mach 4 Flight Conditions in the LENS II Test Facility," 30th JANNAF Meeting, Boston, MA, May 12-16, 2008.

19. Holden, M.S., Mundy, E.P., and Wadhams, T.P., "A Review of Experimental and Analytical Studies of Roughness, Blowing, and Roughness with Blowing on Hemispherical and Conical Shapes at High Mach Numbers," AIAA 2008-3907, 38th AIAA Fluid Dynamics Conference & Exhibit, Seattle, WA, June 23-26, 2008.

20. Holden, M.S., Wadhams, T.P., MacLean, M., Mundy, E., "Review of Studies of Boundary Layer Transition in Hypersonic Flows over Axisymmetric and Elliptic Cones conducted in the CUBRC Shock Tunnels," AIAA Paper 2009-0782, Orlando, FL, January 2009.

21. Holden, M., Mundy, E., Wadhams, T., and MacLean, M., "Boundary Layer Transition, Roughness and Blowing Effects on Aerothermal Characteristics of Hemispherical Heat Shields," AIAA 2010-1066, 48th AIAA Aerospace Sciences Meeting, Orlando, FL, January 4-7, 2010.

22. Wadhams, T., MacLean, M., and Holden, M., "A Review of Transition Studies on Full-Scale Flight Vehicles at Duplicated Flight Conditions in the LENS Tunnels and Comparisons with Prediction Methods and Flight Measurements," AIAA 2010-1246, 48th AIAA Aerospace Sciences Meeting, Orlando, FL, January 4-7, 2010.

23. Holden, M., Harvey, J., Wadhams, T., and MacLean, M., "A Review of Experimental Studies with the Double Cone Configuration in the LENS Hypervelocity Tunnels and Comparisons with Navier-Stokes and DSMC Computations," AIAA 2010-1281, 48th AIAA Aerospace Sciences Meeting, Orlando, FL, January 4-7, 2010.

24. Parker, R., Holden, M. and Wakeman, T., "Shock Front Radiation Studies at CUBRC," AIAA 2010-1370, 48th AIAA Aerospace Sciences Meeting, Orlando, FL, January 4-7, 2010.

25. MacLean, M., Dufrene, A., Wadhams, T. and Holden, M., "Numerical and Experimental Characterization of High Enthalpy Flow n an Expansion Tunnel Facility," AIAA 2010-1562, 48th AIAA Aerospace Sciences Meeting, Orlando, FL, January 4-7, 2010.